

**ANALYSES OF ISOTHERMAL SOLIDIFICATION KINETICS DURING  
TRANSIENT LIQUID PHASE BONDING OF SILVER WITH  
ALUMINIUM AND COPPER FILLER METALS**

**By**

**DEBORAH EBUNOLUWA MICHAEL**

A thesis submitted to the Faculty of Graduate Studies in partial fulfillment of the requirements

for the degree of

**MASTER OF SCIENCE**

Department of Mechanical Engineering

University of Manitoba

Winnipeg, Manitoba,

Canada

## **ACKNOWLEDGEMENT**

I sincerely thank my advisor, Dr. Olanrewaju Ojo, for the privilege of successfully completing my post-graduate study under his capable supervision. I appreciate his guidance, consistent support, words of encouragement, and invaluable contribution towards my research work. I would also like to thank the laboratory technicians, Trevor Smith and Mike Boskwick, for their assistance.

My gratitude goes out to my friends and colleagues for their support throughout my master's program: Francis Amushi, Oluyemi Aina, Gbenga Asala, Nnaemeka Ugodilinwa, Amin Ghanbar, Sanmi Oguntuase, James Adu, Dr. Osoba, Dr. Lina, Jamiu Mojolagbe, Emmanuel Adejumo, Chidinma Anyanwu, Taiwo Dada, and Hassan Oyelaja.

This journey would have been impossible without the unconditional love, prayers, and all-round support of my family; thanks to my amazing mom and dad – Mr. and Mrs. Michael Odebode – and my awesome siblings – Lydia and Lois Michael.

Finally, I return all glory to the Almighty God for the strength, wisdom, knowledge, insight, and ability to complete my master's program and to write this thesis. I am deeply grateful!

## ABSTRACT

Transient Liquid Phase Bonding (TLP) is a high temperature joining process that is used for bonding advanced materials that are generally difficult to weld by conventional welding techniques. This study is designed to adequately examine the effect of the key process parameters, such as the bonding time and temperature, on the kinetics of isothermal solidification during TLP bonding. The TLP bonding experiments are carried out in a vacuum furnace under a vacuum pressure of  $5 \times 10^{-5}$  torr at temperatures of 790°C, 820°C, and 850°C. The results show that a deviation from the parabolic law occurred during the isothermal solidification process, at all the selected bonding temperatures. This deviation from the parabolic law cannot be explained by the existing concepts suggested in the literature. In this research work, qualitative and quantitative analyses of the concentration profiles of the experimental samples reveal that the diffusion coefficient is a function of concentration and time, which is in contrast to the general assumption of a constant diffusion coefficient. This important experimental finding, which has not been previously reported in the literature during TLP bonding, can explain the occurrence of a deviation from the parabolic law. Furthermore, the experimental results show that an increase in the bonding temperature results in an increase in the rate of isothermal solidification, due to increased diffusivity of the MPD solutes with increase in temperature. Notwithstanding, larger residual liquid is observed at higher bonding temperatures; this is attributed to the overriding effect of the increase in the volume of the liquid phase at the joint when temperature is increased.

# Contents

ACKNOWLEDGEMENT .....	ii
ABSTRACT .....	iii
List of Tables .....	vi
List of Figures .....	vii
1. INTRODUCTION .....	1
1.1. Background Information .....	1
1.1.1. Importance of Joining .....	1
1.1.2. Joining Techniques .....	1
1.1.3. TLP Bonding.....	3
1.2. Motivation .....	4
1.3. Research Objective.....	5
1.4. Major Findings .....	5
1.5. Thesis Structure.....	7
2. LITERATURE REVIEW .....	8
2.1. Brazing .....	8
2.1.1. General Description .....	8
2.1.2. Advantages.....	10
2.1.3. Limitations .....	10
2.1.4. Brazing Techniques .....	11
2.1.5. Selection of Filler Metals.....	18
2.1.6. Brazing Fluxes .....	19
2.1.7. Surface Preparation.....	20
2.1.8. Brazing Atmosphere .....	21
2.2. Transient Liquid Phase (TLP) Bonding .....	22
2.2.1. TLP Bonding Background .....	22
2.2.2. Application.....	23
2.2.3. Advantages.....	24
2.2.4. Disadvantages .....	24
2.2.5. Process Description.....	25
2.2.6. Kinetics of TLP bonding.....	26
2.2.7. Selection of TLP bonding process parameters.....	34

2.3. Research Scope .....	36
3. MATERIALS AND EXPERIMENTAL PROCEDURE .....	37
3.1. Materials.....	37
3.1.1. Material Systems.....	37
3.1.2. Base Materials.....	37
3.1.3. Filler Material .....	37
3.2. Sample Preparation .....	39
3.2.1. Bonding Coupons Fabrication .....	39
3.2.2. Interlayer Foil Preparation .....	39
3.2.3. Substrate Coating .....	39
3.3. Experimental Setup .....	41
3.3.1. Equipment.....	41
3.3.2. Sample Assembly and TLP Bonding.....	41
3.3.3. Microscopic Examination .....	43
4. RESULTS AND DISCUSSION.....	44
4.1. Effect of Holding Time on the Kinetics of TLP Bonding.....	44
4.1.1. Ternary System – Ag Al-Cu Ag.....	44
4.1.2. Binary System – Ag Cu Ag.....	51
4.1.3. Quantitative Evaluation of Variable Diffusion Coefficient Using Hall’s Method .	69
4.2. Effect of bonding temperature on the kinetics of TLP bonding process.....	75
5. CONCLUSIONS AND SUGGESTIONS FOR FUTURE WORK.....	82
5.1. Conclusions .....	82
5.2. Suggestions for Future Work .....	84
REFERENCES .....	85

## List of Tables

Table 3.1: Physical properties of as-cast silver .....	38
--	----

## List of Figures

Figure 2.1: Types of braze joint configuration [12].....	9
Figure 2.2: Schematic illustration of laser brazing.....	16
Figure 2.3: Ag-Cu binary phase diagram [45].....	27
Figure 2.4: Dissolution of base metal and widening of liquid phase during TLP bonding [38].....	29
Figure 2.5: Isothermal solidification of liquid phase during TLP bonding [38] .....	31
Figure 2.6: Homogenization of the joint after complete isothermal solidification [38].....	33
Figure 3.1: Ternary system stacking sequence .....	40
Figure 3.2: Thermal cycle used for TLP bonding .....	42
Figure 4.1: Microstructure showing the distinct regions across TLP bonded Ag Al-Cu Ag system.....	45
Figure 4.2: Plot of average eutectic width against square-root of time for Ag Al-Cu Ag samples bonded at 820°C.....	48
Figure 4.3: Concentration profile of Cu – with its origin starting from the solid/liquid interface – for Ag Al-Cu Ag sample bonded at 820°C for 96 hours .....	50
Figure 4.4: SEM micrograph showing the typical microstructure of TLP bonded Ag Cu Ag system.....	52
Figure 4.5: Plot of average eutectic width against square-root of time for Ag Cu Ag bonded at 820°C..	53
Figure 4.6: Plot of average eutectic width against square-root of time for Ag Al-Cu Ag and Ag Cu Ag .	54
Figure 4.7: Plot of average eutectic width against square-root of time for Ag Cu Ag at temperatures of 790°C, 820°C, and 850°C.....	57
Figure 4.8: (a) 1 hour and (b) 96 hours SEM micrographs showing the grains in the region adjacent to the solid/liquid interface for Ag Cu Ag samples bonded at 850°C.....	58
Figure 4.9: Concentration profile of Cu – with its origin starting from the solid/liquid interface – for Ag Cu Ag samples bonded at 790°C and held for times ranging from 1 hour to 96 hours .....	61

Figure 4.10: Concentration profile of Cu – with its origin starting from the solid/liquid interface – for Ag Cu Ag samples bonded at 820°C and held for times ranging from 1 hour to 96 hours.....	62
Figure 4.11: Concentration profile of Cu – with its origin starting from the solid/liquid interface – for Ag Cu Ag samples bonded at 850°C and held for times ranging from 1 hour to 96 hours.....	63
Figure 4.12: Expected trend of the concentration profiles when $D=f(C)$ is not changing with time.....	65
Figure 4.13: Concentration profile of Cu plotted on a normalized x-axis for Ag Cu Ag samples bonded at 790°C and held for times ranging from 1 hour to 96 hours.....	66
Figure 4.14: Concentration profile of Cu plotted on a normalized x-axis for Ag Cu Ag samples bonded at 820°C and held for times ranging from 1 hour to 96 hours.....	67
Figure 4.15: Concentration profile of Cu plotted on a normalized x-axis for Ag Cu Ag samples bonded at 850°C and held for times ranging from 1 hour to 96 hours.....	68
Figure 4.16: Probability plot of $c/c_0$ against $\lambda$ for Ag Cu Ag at 820°C.....	70
Figure 4.17: Plot of diffusion coefficient against concentration at 790°C for 1 hour, 15 hours, and 72 hours.....	72
Figure 4.18: Plot of diffusion coefficient against concentration at 820°C for 1 hour, 15 hours, and 72 hours.....	73
Figure 4.19: Plot of diffusion coefficient against concentration at 850°C for 1 hour, 15 hours, and 72 hours.....	74
Figure 4.20: Plot of diffusion depth against the bonding temperature.....	76
Figure 4.21: Plot of rate of isothermal solidification against temperature.....	78
Figure 4.22: Plot of maximum width of liquid against temperature.....	80
Figure 4.23: Plot of time required for complete isothermal solidification against temperature.....	81

# 1. INTRODUCTION

## 1.1. Background Information

### 1.1.1. Importance of Joining

The satisfactory performance of any engineering structure requires continuous maintenance of its structural integrity [1]. Mechanical structures are continually subject to static and dynamic loadings. These loadings induce stresses that are liable to cause structural deformation or damage. When a structure is damaged, the load carrying capacity decreases permanently [2]. Therefore, the need for a suitable and economical method of repairing damaged structures is of utmost importance. Additionally, the increasing complexity of engineering components also makes fabrication difficult. Hence, the need to efficiently fabricate complex structures and repair damaged parts by joining cannot be overemphasized. It is imperative that structural parts be joined according to the best available techniques because inappropriate joining techniques can pose an immediate or potential danger [1].

### 1.1.2. Joining Techniques

Traditional welding methods, classified into three categories – fusion welding, non-fusion welding, and cold welding – are the most commonly used joining techniques [3], [4]. In fusion welding, the adjacent areas of the materials to be joined are heated up to molten state and subsequently cooled to achieve the weld. The weldment usually consists of three different regions, which are: the fusion zone, i.e. the region that undergoes melting and solidification, the Heat Affected Zone (HAZ) which suffers significant thermal exposure, thereby serving as a

crack initiation site, and the base metal; this region is unaffected by the welding process [5]. Non-fusion welding processes achieve welding by heating up the pair of materials to be joined to a semi-molten state, and subsequently applying pressure, which causes the pair of materials to interlock at the joint interface by plastic deformation. Chemical bonds are formed at the joint and a weld is produced [6], [7]. Cold welding is a solid-state process where sufficient pressure is applied to the materials at room temperature, to produce intermolecular bonding of the metals with substantial plastic deformation at the weld [7].

Non-fusion welding and cold-welding processes are suitable for soft or ductile materials while fusion welding is extensively used to join advanced materials in the aerospace, automotive, biomedical and power generation industries. Nevertheless, the formation of HAZ in the weldment puts a limitation on the effectiveness of this process because, not only does the HAZ serve as a crack initiation site, it degrades the mechanical properties of the joint [8], thereby, reducing the lifespan of the structure. Additionally, fusion welding is not suitable for joining structures with complex geometries. Also, the equipment needed for fusion welding processes are expensive and the process is time consuming [9].

An alternative to the conventional welding methods is brazing. Brazing is a method of joining materials with the use of a filler metal, and it is usually carried out at temperatures above 450°C, without adversely affecting the integrity of the base metals (aka substrates). The brazing temperature is selected within the liquidus of the filler material, but at the solidus of the substrate materials [10]. During this joining process, only the filler material melts. The molten filler wets the adjoining surfaces of the substrates, and is then cooled to join the substrate materials together [11]. This process differs significantly from welding where it involves the melting and recrystallization of the substrates by applying heat, pressure, or a combination of both. The

commonly used filler metals are either pure or alloys of silver (Ag), aluminum (Al), copper (Cu), gold (Au), nickel (Ni), or cobalt (Co). Brazing is production and cost effective. It can be used to join dissimilar materials as well as thick or thin materials. Additionally, only minimal labor is required for the entire process [12]. The major downside to brazing is the formation of a non-equilibrium eutectic-type solidification reaction product on cooling, which is detrimental to the joint. Paulonis et al. [13] developed a new joining technique known as Transient Liquid Phase (TLP) bonding, also called diffusion bonding, which combines the beneficial features of brazing and eliminates the eutectic by allowing for diffusion of the molten filler (aka interlayer) into the substrates. These advantageous features have made TLP bonding an attractive joining method for efficiently joining advanced materials for use in a wide range of aerospace, biomedical, and electronics applications, without causing any damage to their structural integrity.

### **1.1.3. TLP Bonding**

TLP bonding involves inserting an interlayer material between a pair of substrates and heating up the sandwich structure to a chosen bonding temperature. The assembly is held at the bonding temperature for a specified amount of time, to isothermally solidify. The interlayer is required to have its melting point below that of the substrate materials being joined; therefore, the interlayer is usually an alloy containing melting point depressants (MPD). The bonding temperature is selected so that an equilibrium liquid is formed at the joint through eutectic reaction between the interlayer and the substrates. The interlayer material melts first and rapidly attain equilibrium with the substrate materials through melt back (dissolution) of the adjoining areas of the substrates.

Subsequent diffusion of the MPD solutes from the liquid into the substrates on reaching the bonding temperature initiates isothermal solidification. The diffusion process is continuous, and the volume of the liquid reduces gradually to maintain equilibrium, until the liquid is completely used up. The effectiveness of TLP bonding depends on the process parameters, such as the holding time, bonding temperature, and gap size. To achieve a time efficient process and produce joints with acceptable quality, the process parameters must be optimized for elimination of the liquid in the joint by complete isothermal solidification.

## **1.2. Motivation**

TLP bonding largely involves the process of isothermal solidification of the liquid phase formed at the joint, which is controlled by the diffusion of solutes from the liquid into the substrates. Numerous investigations have been carried out to study the effect of the process parameters on isothermal solidification [14]–[18]. There are some agreements in the literature on how the kinetic of the isothermal solidification process is affected by the selected parameters; nevertheless, there are some contradictions in a number of findings reported in the literature. Presently, there are no satisfactory explanations to the contradictory trends reported by various researchers; for instance, the findings in [19], [20] show that increasing the bonding temperature will quickly eliminate the liquid zone at the joint. This is because the diffusivity of the MPD solutes increases with increase in temperature. However, other studies [21], [22] reported otherwise. Furthermore, the isothermal solidification process is generally reported to follow the parabolic law, where the lateral displacement of the solid/liquid interface is proportional to the square-root of time. But contrary to this expectation, some studies report a deviation from the parabolic law.

One of the crucial factors limiting proper analysis of TLP bonding results, which would be greatly beneficial to understanding the process better, is the nature of the MPD element used for experimental investigations. A large number of TLP bonding studies use Boron (B) as the melting point depressant. This element is extremely hard to quantify by the common spectroscopy method because it is a very light element. Therefore, this research was initiated to better understand the influence of key process parameters, specifically bonding temperature and holding time, on isothermal solidification during TLP bonding by designing a system where the concentration of the MPD element can be easily detected and quantified using Energy Dispersive X-ray Spectroscopy (EDS) technique.

### **1.3. Research Objective**

The objective of this research is to study the influence of temperature and time on isothermal solidification behavior during transient liquid phase bonding of Ag metal substrates using Al and Cu as the interlayer materials.

### **1.4. Major Findings**

To achieve the objective of this study, TLP bonding of ternary and binary systems is conducted; Ag substrates are bonded using Al and Cu interlayer materials. The experiments are carried out in a vacuum furnace under a pressure of  $5 \times 10^{-5}$  torr.

The ternary system, Ag|Cu|Ag, is bonded at a temperature of 820°C for holding times ranging from 1 hour to 96 hours. The experimental results show that a deviation from the parabolic law occurred during isothermal solidification of the liquid phase in the joint. The concentration profiles of the samples show that Cu is the only solute actively diffusing from the molten

interlayer into the substrates. It is reported in the literature that the deviation from parabolic law during isothermal solidification is likely due to the presence of a second solute in the interlayer. However, in contrast to this report, the results of this study show that a deviation from the parabolic law can occur without a second solute present in the interlayer.

A different set of experiments are done using Ag|Cu|Ag binary system; the samples are bonded at temperatures of 790°C, 820°C, and 850°C to further investigate the effect of holding time and bonding temperature on the elimination of the liquid phase in the joint. Similar to the trend observed during bonding of the ternary system, the experimental results show that a deviation from the parabolic law occurred at the three temperature conditions. Some studies report that a deviation from the parabolic law is due to the formation of second phase precipitates or can be attributed to grain growth during isothermal solidification; however, in this study, microscopic examination of the bonded samples reveals that there was no formation of second phase precipitates, and that the grain sizes are comparable throughout the isothermal solidification process. It is observed from the concentration profiles of the bonded Ag|Cu|Ag samples that the diffusion coefficient varies with concentration and time. This change in diffusion coefficient with concentration and time can explain the deviation from the parabolic law.

Furthermore, the experimental results show that an increase in the bonding temperature results in an increase in the rate of isothermal solidification, due to increased diffusivity with increase in temperature. Nevertheless, a larger residual liquid is observed at higher temperatures. This contrast in behavior is attributable to the increase in the volume of the liquid phase at the joint when temperature is increased i.e. there is more liquid in the joint to be used up during isothermal solidification, which nullifies the increase in the rate of isothermal solidification when temperature is increased.

## 1.5. Thesis Structure

This thesis was organized as follows:

- An introduction, which includes the background information, motivation for the research, the research objective, major findings, and the thesis structure, is given in Chapter 1.
- In Chapter 2, an extensive literature review on the different brazing techniques, the suitable atmospheres for carrying out brazing, as well as the advantages and disadvantages of the joining process is provided. The chapter also discusses the basic concepts of TLP bonding and how the entire process is affected by certain process parameters.
- The material systems used for experimental investigations, the sample preparation techniques, and the equipment used are listed in Chapter 3. The methods used for analysis of the results obtained in this study are also outlined in this chapter.
- The analysis of the results obtained from the TLP bonded systems are reported in Chapter 4. The effect of holding time and bonding temperature on TLP bonding are discussed. Details of the effect of a variable diffusion coefficient on the bonding process, which explains the anomalies observed during TLP bonding, are given in this chapter. Experimental and theoretical explanations that resolve the conflicting trends associated with increase in temperature are also provided.
- The summary of this research work and some recommendations for future investigations are highlighted in Chapter 5.

## **2. LITERATURE REVIEW**

### **2.1. Brazing**

#### **2.1.1. General Description**

Brazing is a technique for joining metal parts with the use of a filler metal and by the application of heat, usually at temperatures above 450°C. The filler metal, which is required to have a melting temperature lower than those of the metals to be joined, is either pre-placed or fed into the joint by capillary force while the assembly is being heated. The resulting molten zone in the joint on heating, is cooled to room temperature to join the workpieces together. The concept of joining two metals by brazing dates back to 4000 B.C, where gold and silver brazing were carried out by Sumerians in Western Asia [23], [24].

The mostly used fillers materials are either pure or alloys of Al, Au, Ag, Cu, Co, and Mg, which are available in various forms such as powder, paste, foil, wire or rod, and tape. Several types of braze joint configuration include butt joint, lap joint, butt-lap joint, scarf joint and tee joint as shown in Figure 2.1. Before brazing, the materials to be joined are cleaned with a flux to prevent oxidation of the base and filler materials. The flux facilitates wetting of the metal surfaces by the molten filler by dissolving the oxides present on the metal surfaces, and also, acts as an oxygen barrier by coating the hot surfaces. Some of the earliest known fluxes are naturally-occurring soda, lime, lead sulfide, charcoal and other alkalis [12], [25].

This item has been removed due to  
copyright issues. To view it go to:



[https://www.oerlikon.com/.../oerlikon\\_BRO-0010.4\\_Introduction\\_to\\_Brazing\\_EN.pdf](https://www.oerlikon.com/.../oerlikon_BRO-0010.4_Introduction_to_Brazing_EN.pdf)

*Figure 2.1: Types of braze joint configuration [12]*

### **2.1.2. Advantages**

Brazing has various beneficial features such as [10], [26]:

- It is cost effective and assemblies can be processed in batches
- It can be used to join both similar and dissimilar materials of different thicknesses and sizes
- It is a flexible technique that can be adapted to various nonmetal-to-metal combinations
- The thermal cycle is benign, bulk melting of the base metals is prevented and local distortion is minimized or eliminated
- It possesses exceptional stress distribution and heat-transfer properties
- The ability to preserve distinct metallurgical characteristics of metals
- Reproducible and reliable quality control methods.

### **2.1.3. Limitations**

Some major drawbacks of brazing are [27]:

- The formation of a heterogeneous joint composed of the different phases with differing physical and chemical properties
- The lack of joint strength owing to the use of soft filler materials
- Brazed joints can be easily damaged under high service temperatures
- The need to use suitable fluxing agents to maintain cleanliness of the metals
- Aesthetic disadvantage – the color of the joint is usually different from the base metals.

#### **2.1.4. Brazing Techniques**

Effective brazing requires efficient transfer of heat from the heat source to the joint of the assembly. Therefore, the brazing method employed for any joining process is dependent on several factors, such as the complexity and size of the components to be joined, the production rate, the thermal cycle, and the heating and cooling rate. These factors differ significantly with different heating methods used for brazing. The heating methods are categorized into six commonly used methods:

- Torch brazing
- Furnace brazing
- Induction brazing
- Dip brazing
- Resistance brazing
- Infrared brazing

And four lesser known heating methods [10]:

- Laser brazing
- Exothermic brazing
- Weld brazing
- Microwave brazing

##### **2.1.4.1. Torch brazing**

This is a widely used mechanized method of brazing that is ideal for small and short-run production, hard-to-reach applications requiring a manual torch, and some specialized

operations. In torch brazing, the joint of the assembly is heated using a hot gas torch and because the melting point of the filler material is usually lower than that of the base metals but within their oxidizing temperatures, a flux is employed during the process to prevent oxidation of the joint. The hot gas is generated by combustion of oxygen and a fuel gas (i.e. oxyfuel combustion). There are three types of torch brazing; the manual method, which employs the use of a hand-held or fixed position torch – this is a labor-intensive method because it mostly requires the use of human power and skills. The machine method employs both manual and automatic processes – the torch is held by an automated machine while an operator controls the placement/movement of the assembly. Lastly, the automatic method – the operator only loads and unloads the assembly. The entire process is fully mechanized and has a higher production rate than the other two methods [28].

#### **2.1.4.2. Furnace brazing**

This method of brazing was first commercialized in the early 1920's, a furnace is the heat source used to heat the components to be joined to the brazing temperature until the filler material wets the adjoining surfaces of the base metals. The joint is then cooled in a separate chamber to achieve the braze. Brazing furnaces are either gas-fired or electrically heated. Furnace brazing is the most versatile of all brazing processes and it allows for economic production of large batches of components. The protective atmosphere in the furnace enables materials to be processed without aesthetic damage. There are different types of protective atmosphere used but they are mainly divided into two categories namely, gaseous atmosphere and vacuum [29], [30].

#### **2.1.4.3. Induction brazing**

Induction brazing can only be applied when at least one of the components to be joined is ferromagnetic because the process employs the use of electricity through an induction coil to heat up the joint of the assembly. The conducting materials are held at the center of an induction coil and a medium or high frequency alternating current is passed through the coil. This creates a magnetic field around the coil, which causes current to flow to the surface of the materials and heat them up. The filler material melts by rapid heating of the joint area to which it has been applied. In this brazing process, heating is localized to the surfaces near the joint, which is a major advantage especially with components that allow minimal to no distortion and where metallurgical changes are not permissible [10], [31].

#### **2.1.4.4. Dip brazing**

During dip brazing, the components to be joined are assembled and pre-heated in an air furnace and subsequently immersed in a heated bath of molten metal or a flux bath of molten salt. The molten filler metal flows into the gap between the base components by means of capillary action. The assembly is removed from the bath and left to cool. Strong, uniform, and leak-proof joints are produced through this brazing process. Irrespective of the number of joints in one assembly, the joining process is performed in one dip, thus saving time and minimizing cost. Dip brazing is commonly used as an alternative to soldering for manufacturing electronics and small components [32].

#### **2.1.4.5. Resistance brazing**

Resistance brazing is quite different from the other brazing methods in the sense that a molten filler cannot be fed into the joint by capillary action. Rather, a filler material has to be pre-placed

in-between the joint; it can be in the form of a foil, paste or sometimes electroplated on the surfaces of the base materials. This is because this method of brazing requires that the mating components be in intimate contact during the heating and brazing process. The use of a flux which can hinder intimacy is usually eliminated and instead, a self-fluxing filler material such as Silicon-Phosphorous alloys is used. Resistance brazing is usually applied to joints with high electrical conductivity. The assembly – consisting of the parts to be joined and the pre-placed filler material – is part of an electrical circuit. A direct current is then sent through the base materials. The heat that melts the filler alloy is generated either from the resistance of the base materials to the flow of electricity or from a high-resistance electrode placed in contact with the joint [10], [33].

#### ***2.1.4.6. Infrared brazing***

In infrared brazing, heat is generated by light radiation below the visible red rays in the spectrum. The invisible radiation (i.e. infrared energy) is produced from high-intensity quartz incandescent lamps. Infrared brazing is similar to furnace brazing, the only significant difference is the source of heat used to carry out the brazing process. The assembly of components to be joined is locally heated by the infrared rays produced. The heating takes place very rapidly and brazing is typically achieved within seconds. The heat supplied to an assembly varies inversely as the square of distance to the heat source which are the lamps. This is a highly potential joining technique with the advantages of rapid thermal cycle, low energy consumption, no need for vacuum, low cost, easy operation and negligible distortion of the metallurgical properties of the base materials [10].

#### **2.1.4.7. *Laser brazing***

Laser brazing is a rarely used method of brazing, it is used only in applications where a small or localized area of heat is required. The heat for brazing is generated by a laser beam. This method of joining is mostly used for joining galvanized metal sheet but can also be used to braze other materials. It is usually employed in the automotive industry to join or fill the gap between two steel sheets as schematically shown in Figure 2.2. The laser beam is applied directly to a filler material. The filler melts, wets the surfaces of the sheets and joins them together after being allowed to solidify. Some of the advantages of this process are: good quality joint with high-strength seam, low heat input and therefore no distortion of the base materials, reliability of the seam and high productivity. While some of the drawbacks are: high investment cost, narrow part tolerances, laser safety requirements and novelty of the process [34], [35].

This item has been removed due to  
copyright issues. To view it go to:



<http://www.ionix.fi/en/technologies/laser-processing/laser-brazing/>

*Figure 2.2: Schematic illustration of laser brazing*

#### **2.1.4.8. Exothermic brazing**

Exothermic brazing as the name implies uses exothermic reactions between the materials to be joined to achieve a braze. An exothermic reaction is a chemical reaction between two or more reactants in which heat is given off due to the free energy of the system i.e. the system releases energy by heat. This type of brazing involves the use of a pre-placed filler metal. The heat required to melt the filler metal and wet the surfaces of the components being joined is generated by a solid-state metal-to-metal chemical reaction. Exothermic brazing employs simplified tooling and equipment. It can be used to join small components to large structures, for joining honeycomb sandwich panels and to make tube connections for hydraulic lines in aircrafts. Some of the major advantages are the production of reliable and reproducible joints, and it is a relatively simple and economical technique [10].

#### **2.1.4.9. Weld brazing**

Weld brazing process are similar to arc welding, the difference lies mainly in the melting point of the filler material, which is significantly lower than that of the base materials. This method is excellent for joining similar and dissimilar materials, galvanized thin steel sheets and offers considerably greater possibilities for joining composite materials. Weld brazing is carried out in projection welding machines using mostly bronze, brass or aluminum fillers. It combines heating with a passing current and compression of the joint to achieve a braze. Weld brazing is a low-temperature alternative to welding. It is a low-cost method that provides good joint strength and the brazing can be completed in a very short time [10].

#### **2.1.4.10. Microwave brazing**

Microwave brazing is a relatively new brazing process used for joining ceramics parts or ceramic-to-metal dissimilar material parts. This process is hardly used for metal-to-metal combinations because it was observed that ceramics absorb microwave energy more efficiently than base metals. The assembly consisting of ceramic components and a filler material is placed in a microwave reactor and localized heating of the joint by microwave radiation melts the filler material. Microwave brazing has various potential applications including cutting tools, turbine blades, electronic devices and so on but the process is still undergoing development and it is yet to be fully explored [10].

#### **2.1.5. Selection of Filler Metals**

An appropriate selection of a filler metal is necessary to achieve satisfactory brazed joints. When selecting a brazing filler, the key factors to be considered include the brazing process being employed, the atmosphere, the brazing temperature, the heating rate, the design of the joint and the method of applying the filler metal. Other vital factors include the ability of the filler metal to alloy or combine with the base materials being joined, the fluidity at the brazing temperatures to ensure flow by capillary action and wetting of the adjoining surfaces of the base materials, low volatilization of alloying elements of the brazing filler metals at brazing temperatures and also, depending on the service requirements, the ability to produce or avoid base metal/filler metal interactions. Some of these factors are determined by the physical properties of the filler metal in the liquid state. An example is wettability of the filler metal which is determined by properties such as density, viscosity and surface tension. Additionally, the liquidus of the filler metal is required to be less than the solidus temperature of the base metals [36].

The most commonly used filler metals are alloys based on silver (Ag), copper (Cu), aluminum (Al), gold (Au), nickel (Ni), titanium (Ti) and magnesium (Mg). These alloys usually contain melting point depressants (MPDs) such as boron, silicon and phosphorous which are added to depress their melting points. These filler metals are available in different forms such as powder, foil, tapes/preforms, paste, wire and rod. Brazing powders are produced by a gas-atomizing process which generates dense, spherical and dry particles containing precise amounts of the elements of the selected alloy. The powders are usually uniform and homogenous. Brazing foils are flexible materials produced by melt spinning technique while the tapes are manufactured by casting a uniform layer of braze alloy and a binder wound in rolls for ease of handling. The brazing paste usually consists of one or a mixture of filler alloy powders and flux-free binder. The binders may either be water or organic based, producing slow or fast drying pastes. Braze wire and rod are binder free, they are usually used in torch brazing and induction brazing applications.

#### **2.1.6. Brazing Fluxes**

Brazing fluxes are used to facilitate wetting of the base materials by the filler metal. Wetting – defined as the flow and spreading of the liquid filler metal on the adjoining surfaces of the solid base materials – not only influences the properties of a brazed joint but is key to the success of any brazing process. Fluxes promote wetting by preventing the formation of surface oxides during heating and dissolving the oxides already present on the base materials and filler metals. They function as an oxygen barrier by forming a thin protective layer over the surfaces of the metals being heated. Fluxes are applied as uniform coatings and they are required to cover and protect the entire mating surfaces until the brazing temperature is reached.

Brazing fluxes are mixtures consisting of varying chemical components. The mixture is blended to ensure easy and smooth application as well as good adherence to the mating surfaces. The chemical components commonly used to manufacture fluxes are: borax, borates, elemental boron, fluoroborates, fluorides, chlorides, alkalis, wetting agents and water. Several filler metals are alloyed with deoxidizing metals such as magnesium, phosphorous or titanium which make them self-fluxing but because these filler metals are only self-fluxing in the molten state, they will oxidize during the heating stage. Therefore, it is necessary to combine the use of prepared fluxes with these fillers [37], [38].

### **2.1.7. Surface Preparation**

Thorough surface preparation before brazing is of vital importance because the production of sound brazed joints is strongly dependent on the nature and quality of the faying surfaces. The presence of grease, wax, oil, dirt or residual oxide films on the surfaces can inhibit wetting and prevent the flow of the molten filler metal. Therefore, it is necessary to carefully clean the base materials and filler metals before brazing. Greases and oils are to be cleaned first before effective removal of oxide layers. There are two major ways to efficiently clean the surfaces of the parts to be brazed:

1. Chemical cleaning is the most effective way of removing all traces of foreign substances. Chemical cleaning agents such as trichloroethylene and trisodium are usually used. Strong oxide films that cannot be removed by these cleaners are eliminated using other chemical cleaning techniques. The selection of chemical cleaning agents depends on several criteria including the nature of the contaminants, the materials being cleaned, the surface condition and the design of the joint.

2. Mechanical cleaning involving abrasive blasting, brushing, blowing, or grinding is another widely used method of removing contaminants and any oxide film from the surfaces of the parts to be joined. The faying surfaces are also slightly roughened by this cleaning process, which enhances capillary attraction and flow of the molten filler metal.

Irrespective of the cleaning agent or the cleaning method used, thorough rinsing of all residue and/or subsequent ultrasonic cleaning of the mating surfaces is required to prevent formation of other undesirable films. Brazing as soon as possible after the materials have been cleaned is usually recommended [10].

#### **2.1.8. Brazing Atmosphere**

The kinetics of oxidation is highly temperature dependent. Therefore, oxygen or moisture present in a joining environment will react with any metallic component being joined to form surface films which impede wetting during the brazing process. Thus, affecting the resulting quality of the brazed joints. Therefore, it is necessary to conduct brazing in a protective environment. The different types of protective atmospheres, classified as gaseous atmospheres, under which brazing can be carried out are as follows [39]:

- *Chemically inert atmospheres* such as argon, helium, nitrogen or vacuum eliminate oxygen and other gaseous elements capable of reacting with the mating surfaces to form surface films which inhibit wetting and the flow of the molten filler metal.
- *Chemically active atmospheres* also known as reducing atmospheres, react with the surface films formed on the base materials and filler metals during the brazing cycle. These atmospheres – hydrogen, carbon monoxide, ammonia, fluorine, and chlorine –

either dissolve and absorb the surface films or react with them to produce compounds that can be easily broken up by the molten filler metal.

Some metals are not compatible with certain gaseous atmospheres and as a result, they can degrade the mechanical properties of the components. Nitrogen atmospheres are not recommended when the base materials and filler metals consist of elements prone to nitriding. The elements combine with nitrogen to form nitrides films on the surface of the components and prevent wetting of the faying surfaces by the molten filler metal. Hydrogen atmospheres can cause hydrogen embrittlement to some metals, thereby lowering the fracture toughness and the strain rate transition between ductile and brittle fracture. Carbon monoxide is poisonous, so, the workstation must be properly vented and continuously monitored for leaks. The presence of ammonia in a brazing atmosphere can result in nitriding of stainless steels and stress cracking of brass.

Controlled gas atmospheres require the use of confining vessels like furnaces which have the advantages of uniform heating of the components, easy automation of the process which allows for batch production and, reduced post-brazing operations such as cleaning and removal of flux residues. To select a suitable brazing atmosphere, each component to be brazed as well as the heating method must be properly assessed [39].

## **2.2. Transient Liquid Phase (TLP) Bonding**

### **2.2.1. TLP Bonding Background**

Transient Liquid Phase bonding is a high quality joining process used to bond similar or dissimilar materials. This method dates back to ancient times. It was known as granulation in the

sixteenth century and was used for attaching decorative gold beads to ceremonial articles [40]. The joining process was modified and renamed as TLP bonding about half a decade ago by Paulonis et al. [13].

Like brazing, TLP bonding relies on the formation of a liquid phase at the joint by an interlayer that melts at a temperature lower than the melting point of the base materials. However, the most beneficial feature of this process which differentiates it from the brazing processes is the re-solidification of the liquid at a constant temperature i.e. isothermal solidification of the liquid phase. The interlayer contains a melting point depressant (MPD). Upon heating of the assembly to the bonding temperature, it melts or reacts with the base materials to form a liquid. The assembly is then held at a constant temperature (above the melting point of the interlayer) until the MPD elements are removed from the liquid phase through solid-state diffusion. The solid/liquid interface recedes while a solid-solution phase is formed as the solute are being lost from the liquid. Isothermal solidification is complete when the two solid/liquid interfaces meet at the joint centerline.

Upon completion of the process, a homogenous bond is formed between the base materials. The re-melt temperature and properties of the joint become similar to those of the base materials [40].

### **2.2.2. Application**

TLP bonding has been successfully employed to join a wide range of materials and structures including Al, Fe, Co, Ni, and Ti-based alloys. It is the most suitable method of joining heat-resistant alloys that are susceptible to hot cracking during welding or post-weld heat treatment. TLP bonding has also been applied to join ceramics, cellular structures, metal matrix composites (MMCs), microelectronics, single crystals, polycrystals, stainless steels, and structural

intermetallics. It is often used in high-stress and high-temperature application where other joining methods such as welding and brazing cannot be used. TLP bonding can be conveniently used to join similar and dissimilar materials [41]. Specific applications include the repair of gas turbine engine components, fabrication of high tolerance parts such as fuel nozzles in combustion chambers, honeycomb seals and thin-walled structures [42].

### **2.2.3. Advantages**

The advantages of TLP bonding include [41]:

- The resulting bonds can operate at the bonding temperature or higher service temperatures i.e. components can be bonded at temperatures equal or lower than the temperatures the joint will be subjected to during service.
- The joints produced have microstructural and mechanical properties similar to those of the base materials.
- The process can tolerate the presence of oxide films on the faying surfaces, therefore the use of fluxes is redundant and only minimal surface/joint preparation is needed.
- Melting of the base materials is minimized, as compared to brazing.
- The liquid phase formed at the joint during TLP bonding fills the voids on uneven mating surfaces thereby, eliminating the need for costly post-bonding processes.
- Several joints can be fabricated simultaneously.
- Overaging of materials that are highly sensitive to temperature is prevented.

### **2.2.4. Disadvantages**

The disadvantages of TLP bonding include [41]:

- The process can take a significantly long time to achieve good quality joints, which is uneconomical in the long run.
- Close fit-up of the mating surfaces is required.
- Rapid heating-up of the assembly is required.
- The formation of a thick layer of intermetallics at the joint interface which can degrade the strength and ductility of the joint.
- The need for post-bond heat treatment of age hardened alloys.

Like every other joining process, TLP bonding has its own disadvantages and certain limitations but it is interesting to know that many of the problems encountered during this process can be fully prevented by optimizing the bonding parameters.

### **2.2.5. Process Description**

TLP bonding process is distinct from brazing and it includes setting up the bond assembly, heating it up to a specified bonding temperature to form a liquid phase in the bond region, holding the assembly at the bonding temperature to allow isothermal solidification of the liquid, which achieved by solid-state diffusion and lastly, homogenization of the bond at an appropriate heat-treating temperature. The bonding assembly is a sandwich structure consisting of an interlayer placed between the base materials. The interlayer is available in different forms such as foils, fine powders, pastes or can even be electroplated on the faying surfaces. The interlayer foil is usually pre-placed in-between the base materials before bonding but when a powdered interlayer is being used, it is placed outside the joint to melt and flow into the joint by capillary attraction. Minimal equilibrium pressure is applied to the assembly to keep each component aligned and to promote bonding by initiating proper contact between the base materials and the

interlayer. Heating of the assembly and homogenization of the bond can be done in a chemically inert atmosphere or a controlled gas atmosphere. However, it is typically carried out in a controlled atmosphere within a confined vessel, usually a vacuum furnace. The assembly is heated in the vacuum furnace under pressure of about 0.00015 mmHg, held for a specific amount of time before allowing to cool and then taken out for post-bonding operations [41].

### **2.2.6. Kinetics of TLP bonding**

Several models have been developed to properly understand the kinetics of TLP bonding process. A simple case is the model [43], [44] proposed for a binary eutectic system where local equilibrium at the interface is assumed between the solid and liquid phases. The composition of each phase is determined by the phase diagram shown in Figure 2.3 with A being the base material and B, the interlayer element. Diverse opinions in the literature have been explored and it has been established that the transient liquid phase bonding process is classified into four major stages namely, the melting of the interlayer, dissolution of the base materials and widening of the liquid, isothermal solidification, and homogenization of the bond region [41], [45].

#### **2.2.6.1. *Melting stage***

During this stage, the assembly is heated from room temperature to the selected bonding temperature, which in most cases is above the melting point of the interlayer to ensure complete melting. However, the interlayer can melt over a range of temperatures above the eutectic temperature – the interlayer begins to melt as a result of eutectic reaction between the interlayer and the base materials. After complete melting, the molten interlayer wets the mating surfaces of the base materials and flows throughout the joint. Wettability as discussed earlier in this chapter,

This item has been removed due to  
copyright issues. To view it go to:



<https://link.springer.com/article/10.1007/BF02649282>

*Figure 2.3: Ag-Cu binary phase diagram [45]*

depends on the viscosity of the liquid and the surface energies of the liquid and base materials [38], [41].

#### **2.2.6.2. *Dissolution and widening stage***

At this second stage, the interlayer has completely melted but heating of the bond region still continues until the bonding temperature is reached. Subsequent interdiffusion between the molten interlayer and the base material occurs, causing changes to the elemental concentration at the solid/liquid interface. The resulting liquid phase at the joint is inhomogeneous and supersaturated, having a solute concentration greater than the liquidus concentration as illustrated in Figure 2.3. Therefore, because the liquid is not in equilibrium with the adjoining solid, it triggers melt-back of the base materials and successive widening of the liquid zone as shown in Figure 2.4. The melt-back and widening process continues until the concentration of the liquid attains the equilibrium value of  $C^{L\alpha}$  and the concentration of the solid adjacent to the liquid becomes equal to  $C^{\alpha L}$  [45]. The extent of dissolution is dependent on the initial thickness of the interlayer, the concentration of the MPD solutes in the interlayer, and the solubility of the solutes in the base materials [38].

This item has been removed due to  
copyright issues. To view it go to:



<http://hdl.handle.net/1993/20938>

*Figure 2.4: Dissolution of base metal and widening of liquid phase during TLP bonding [38]*

### 2.2.6.3. *Isothermal solidification stage*

This stage succeeds the dissolution stage and proceeds at a constant bonding temperature. After the liquid zone at the joint reaches its maximum width, the MPD solutes in the liquid diffuse into the solid base materials at a rate controlled by the diffusion coefficient  $D_s$  (diffusion coefficient of the solute in the solid). Continuous diffusion of the solutes causes the solid/liquid interface to reverse direction and the liquid zone begins to shrink to the center of the joint until it is fully eliminated, provided sufficient holding time is allowed. The isothermal solidification process is illustrated in Figure 2.5. The rate of loss of solutes from the liquid to the base materials controls the interface displacement rate [45].

Standard TLP bonding models confirm that local equilibrium is established and maintained at the solid/liquid interface throughout the isothermal solidification process, keeping the solidus and liquidus concentration fixed at values  $C^{\alpha L}$  and  $C^{L\alpha}$ . The isothermal solidification stage is the most crucial because it is a major determinant of the resulting microstructure of the bond region. Unlike the melting and dissolution stages which take place rapidly and are accomplished in the order of minutes, the time needed to achieve complete isothermal solidification is usually of the order of hours. This stage is much slower than the preceding ones since it is primarily controlled by solid-state diffusion [42].

This item has been removed due to  
copyright issues. To view it go to:



<http://hdl.handle.net/1993/20938>

*Figure 2.5: Isothermal solidification of liquid phase during TLP bonding [38]*

#### **2.2.6.4. Homogenization stage**

This stage takes place after isothermal solidification of the joint and it is illustrated in Figure 2.6. Homogenization can be done at a temperature lower than or above the bonding temperature depending on the sensitivity of the microstructure. The purpose of this stage is to redistribute and even out the solute peak at the joint that remained after isothermal solidification. If sufficient time is allowed for the joint to completely homogenize, no concentration gradient will exist across the joint and the chemistry will be similar to that of the base materials. Hence, the joint's re-melting temperature becomes significantly higher than the melting point of the interlayer and closer to that of the base materials [41].

This item has been removed due to  
copyright issues. To view it go to:



<http://hdl.handle.net/1993/20938>

*Figure 2.6: Homogenization of the joint after complete isothermal solidification [38]*

### **2.2.7. Selection of TLP bonding process parameters**

TLP bonding parameters such as the interlayer material, interlayer thickness, holding time and bonding temperature have a direct influence on the final quality of bonded joints. The aim of this joining process is to produce sound quality joints with their mechanical properties similar to that of the base materials, in a timely and cost-effective manner. To achieve this, the bonding parameters must be well optimized.

#### **2.2.7.1. *Interlayer material***

The composition of the interlayer is an important process parameter that affects the kinetics of process, and the resulting quality of the bonded joint. The dissolution of a pure metal interlayer was said [46] to require a longer time than an alloyed interlayer – the former melts linearly with time while the latter melts instantaneously upon reaching the eutectic temperature. Nevertheless, a suitable interlayer material is required to have strong adherence to the faying surfaces and good fluidity. Additionally, the interlayer is required to contain MPD solutes which have high diffusivity in the base materials and are preferably able to form a solid-solution phase with the base materials.

#### **2.2.7.2. *Interlayer thickness***

For any TLP bonding system, there is a critical interlayer thickness required to achieve a strong bond free of voids in the shortest possible time. The critical thickness is determined by several variables including the bonding temperature, the heating rate and the nature of the base materials. During the initial heating stage, when the interlayer starts to melt, some of the solutes diffuse into the base materials; if the interlayer is too thin, the thickness of the interlayer could significantly reduce or be completely consumed by solid-state diffusion before reaching the

bonding temperature – depending on the diffusion rate and the heating rate. While on the other hand, if the interlayer is too thick, isothermal solidification might take a longer time since there is more liquid present at the joint. Hence, the thickness of the interlayer must be carefully selected to suit the bonding system [41].

#### **2.2.7.3. *Holding time***

The time frame for TLP bonding is an important factor that is highly dependent on the material system (i.e. solubility of the MPD elements in the base materials, their diffusion coefficients, microstructure of the base materials) and the bonding parameters (i.e. interlayer thickness, bonding temperature). Sufficient holding time is needed for complete isothermal solidification of the bulk liquid phase formed at the joint during heating [41]. The relationship between the transient width of the liquid zone and holding time has been said [47], [48] to be linear, following the parabolic rate law. However, in some cases, this has been found to not hold true [49], [50]. Any residual liquid at the joint can form brittle constituents (known as eutectic) on cooling, which has a detrimental effect on the mechanical properties of the joint. Giving adequate time to complete TLP bonding process will allow continuous diffusion of the MPD solutes from the liquid into the base materials until the entire liquid is eliminated [41].

#### **2.2.7.4. *Bonding temperature***

Choosing an optimum temperature for TLP bonding is extremely important because it is one of the major determinants of the rate of isothermal solidification. This choice is made either based on the phase diagram and diffusion data of the material system, if available or determined from experiments. Arrhenius relation:  $D = D_0 \cdot \exp\left(-\frac{Q}{RT}\right)$  shows that the diffusion coefficient increases exponentially with increase in temperature, which could imply that the rate of

isothermal solidification should only increase as temperature is increased, since it is controlled by the rate at which the MPD solutes diffuse into the base materials. Although some studies [19], [20] have reported an increase in the rate of isothermal solidification with increase in bonding temperature, others [21], [22] have reported a reduction in the rate of isothermal solidification as bonding temperature is increased, leading to an increase in the time required for complete isothermal solidification.

### **2.3. Research Scope**

Efficiently joining advanced materials for use in a broad range of aerospace, biomedical, and electronics applications, without damage to their structural integrity has made TLP bonding process an attractive joining method. Various models have been developed to study and improve the kinetics of TLP bonding to make it better suited for industrial applications. Nevertheless, some contradictions still exist in the literature regarding the effect of temperature and holding time on the rate of the process – as discussed in the preceding subsections – and no satisfactory explanations have been given to reconcile the contradictions. Therefore, this research work was carefully designed to study the influence of temperature and time on the elimination of deleterious eutectic microconstituents during transient liquid phase bonding of Ag substrates using Al and Cu as interlayer materials.

The effect of time on the process kinetics is investigated using Ag|Al-Cu|Ag ternary alloy system and Ag|Cu|Ag binary alloy system. TLP bonding of Ag|Cu|Ag was carried out at varying temperatures while keeping other conditions constant to study the effect of bonding temperature on the kinetics of the process.

## **3. MATERIALS AND EXPERIMENTAL PROCEDURE**

### **3.1. Materials**

#### **3.1.1. Material Systems**

To properly analyze the kinetics of TLP bonding process, choosing suitable systems was paramount. The selection criteria used in this research work are:

- I. The systems must have a suitable eutectic region, with the eutectic composition in the base-metal rich zone.
- II. There must be a substantial solubility of the solute in the base metal.
- III. Availability of phase diagram data.

#### **3.1.2. Base Materials**

The base material used for the experimental investigation in this research was commercially pure Ag metal with a purity of 99.95 pct., supplied by Alfa Aesar in the form of 50 mm x 50 mm x 3 mm cast plates. The metal was used in the as-cast condition and the specific physical properties are listed in Table 3.1.

#### **3.1.3. Filler Material**

The filler materials used for the experimental study were commercially pure Cu foils with a purity of 99.99 pct., supplied by Alfa Aesar and Metglass as 127  $\mu\text{m}$  and 25  $\mu\text{m}$  thick foils respectively. In addition, a 25  $\mu\text{m}$  thick Al foil of 99.99 pct. purity supplied by Alfa Aesar was used.

*Table 3.1: Physical properties of as-cast silver*

Density	10.50 g/cm <sup>3</sup>
Melting Point	962°C
Boiling Point	2212°C
Tensile Strength	140 MPa
Poisson's ratio	0.37
Modulus of elasticity	76 GPa

## **3.2. Sample Preparation**

### **3.2.1. Bonding Coupons Fabrication**

The as-received Ag plates were sectioned into rectangular coupons with dimensions of 9 mm x 6mm x 3mm using a computer numerically controlled Electrical Discharge Machine (EDM). The faying surface of the coupons were ground using coarse silicon carbide (SiC) papers with a grit size of 180 to remove the oxide layers and produce a flat surface. The coupons were subsequently cleaned for 15 minutes in an ultrasonic bath using acetone.

### **3.2.2. Interlayer Foil Preparation**

The metal foils were cut to the size of the coupons using a precision knife. The 127  $\mu\text{m}$  Cu foil was used for the binary system experiments. To achieve a ternary system, a Cu-Al alloy foil was needed but was not commercially available. Hence, 25  $\mu\text{m}$  thick Cu and Al foils were used. A 125  $\mu\text{m}$  thick Cu<sub>75</sub>Al<sub>25</sub> filler alloy was achieved by stacking five layers of the 25  $\mu\text{m}$  foils in the sequence illustrated in Figure 3.1.

### **3.2.3. Substrate Coating**

The rectangular coupons are also called substrates. All the sides of the substrates except the faying surfaces were fully coated with a ceramic stop-off. This was designed to prevent spillage of the molten interlayer during bonding in order to maintain a consistent amount of liquid in the joint for all experiments carried out, and also, to maintain the assumption of a planar geometry.

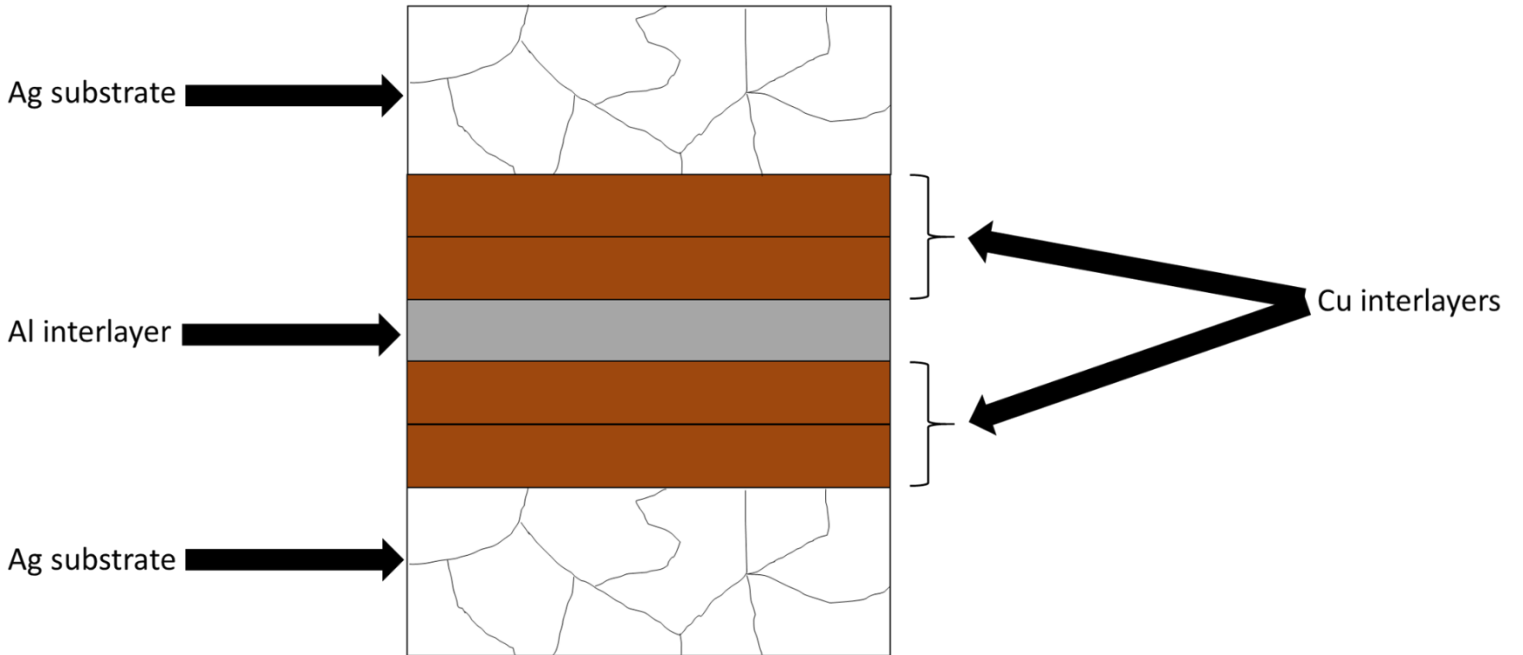


*Figure 3.1: Ternary system stacking sequence*

### **3.3. Experimental Setup**

#### **3.3.1. Equipment**

The equipment used to perform all the TLP bonding experiments was a LABVAC II vacuum furnace. The system is made up of a high temperature vacuum chamber, vacuum pumping system, hybrid controller, gauge controller, and power supply system. The furnace operates under a vacuum pressure of  $5 \times 10^{-5}$  torr to prevent oxidation of the materials being bonded. The heating rate ranges from 0.1 to 20°C/min.

#### **3.3.2. Sample Assembly and TLP Bonding**

The sandwich sample consisting of two coated substrates with the interlayer foil carefully placed and aligned in between the faying surfaces of the substrates is assembled into a fixture. The fixture, also coated with a ceramic stop-off, is equipped with bolts which keeps the assembly in a fixed position during bonding. This is designed to avoid misalignment of the substrates, which can also cause spillage of the molten interlayer during the bonding process. Additionally, Al foil coated with ceramic was used as a guiding frame around the sandwich sample to prevent the flowing out of the molten interlayer from the joint. TLP bonding was carried out by heating the assembly in the vacuum furnace to the bonding temperature and held at that temperature for a given amount of time before cooling to room temperature. The TLP bonding process was carried out using the temperature-time cycle illustrated in Figure 3.2.

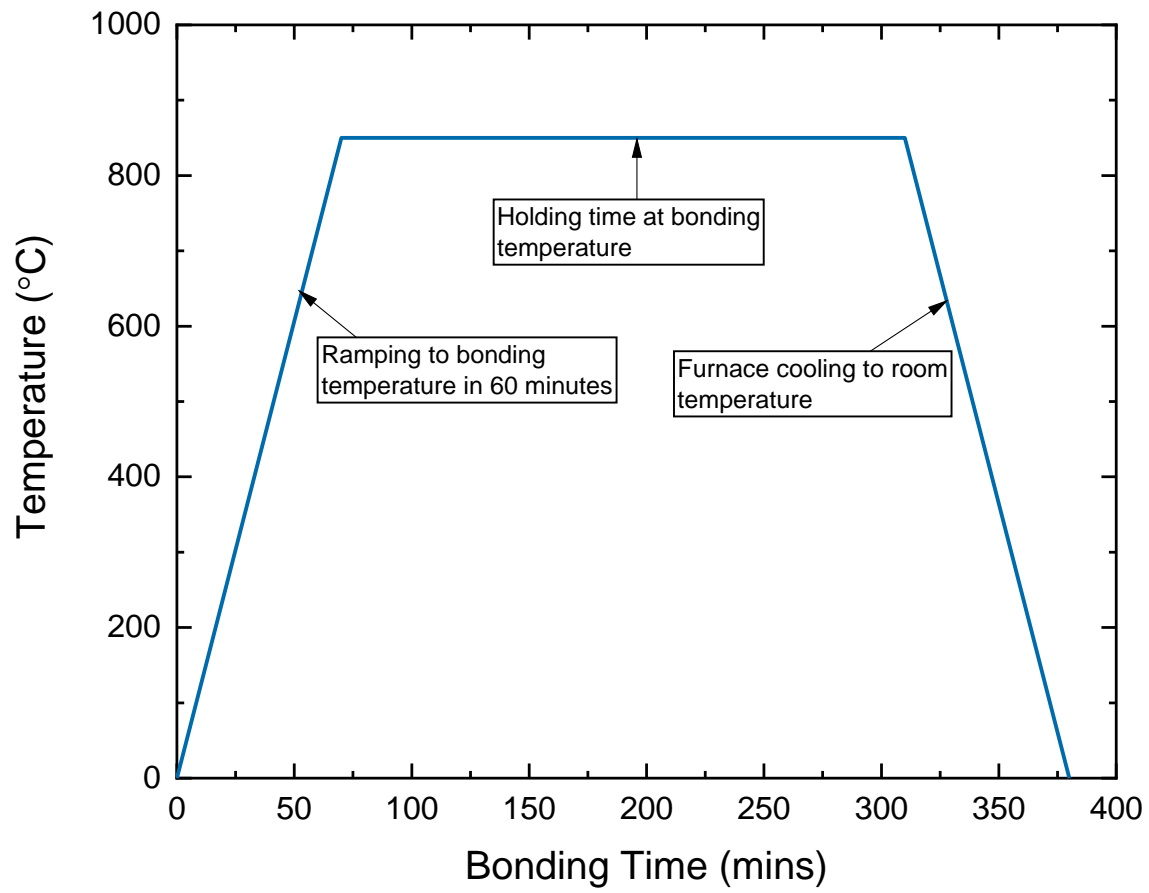


*Figure 3.2: Thermal cycle used for TLP bonding*

### **3.3.3. Microscopic Examination**

The bonded samples were sectioned widthwise – perpendicular to the bonded surfaces using the EDM. The sectioned samples were mounted in bakelite using a Buehler mounting press and subsequently ground with 600 to 1200 grit SiC papers and polished to a 1  $\mu\text{m}$  finish using a diamond suspension fluid. All samples were etched by swabbing using ferric chloride solution. The samples were then cleaned with water before being microscopically examined. The microstructure of the bonded samples was examined using an Inverted Reflected Optical Microscope (OM) equipped with CLEMEX Vision 3.0 image analyzer and a JOEL 5900 Scanning Electron Microscope (SEM) equipped with an ultra-thin window Oxford Energy Dispersive Spectrometer (EDS), which was connected to a computer with INCA analysis software. The joint characterization was done using the OM; the widths of the different regions in the joint were obtained by taking the average of 20 measurements. The EDS was used to obtain the distribution and chemical composition of the diffusing solute.

## 4. RESULTS AND DISCUSSION

In this chapter, the results of the experimental investigations are reported and discussed. They are divided into two sections, namely: the effect of holding time on the kinetics of TLP bonding, and the effect of bonding temperature on the kinetics of TLP bonding.

### 4.1. Effect of Holding Time on the Kinetics of TLP Bonding

#### 4.1.1. Ternary System – Ag|Al-Cu|Ag

TLP bonding of Ag substrates is successfully carried out at a bonding temperature of 820°C using Al-Cu interlayer foils. The holding time is varied from 1 hour to 96 hours. Microstructural examination of the bonded samples shows the formation of eutectic along the joints. Three distinct regions are observed across the joints when the samples are examined using the SEM. Figure 4.1 shows the SEM micrograph of the sample bonded at 820°C for 1 hour. These regions are named as follows: Region I – eutectic, Region II – isothermally solidified zone and Region III – substrates.

**Region I**, referred to as the eutectic, are microconstituents formed due to incomplete isothermal solidification of the liquid phase at the joint. When adequate time is not allowed for complete diffusion of the solutes into the adjoining substrates, the residual liquid in the joint forms these microconstituents during cooling from the bonding temperature to room temperature.

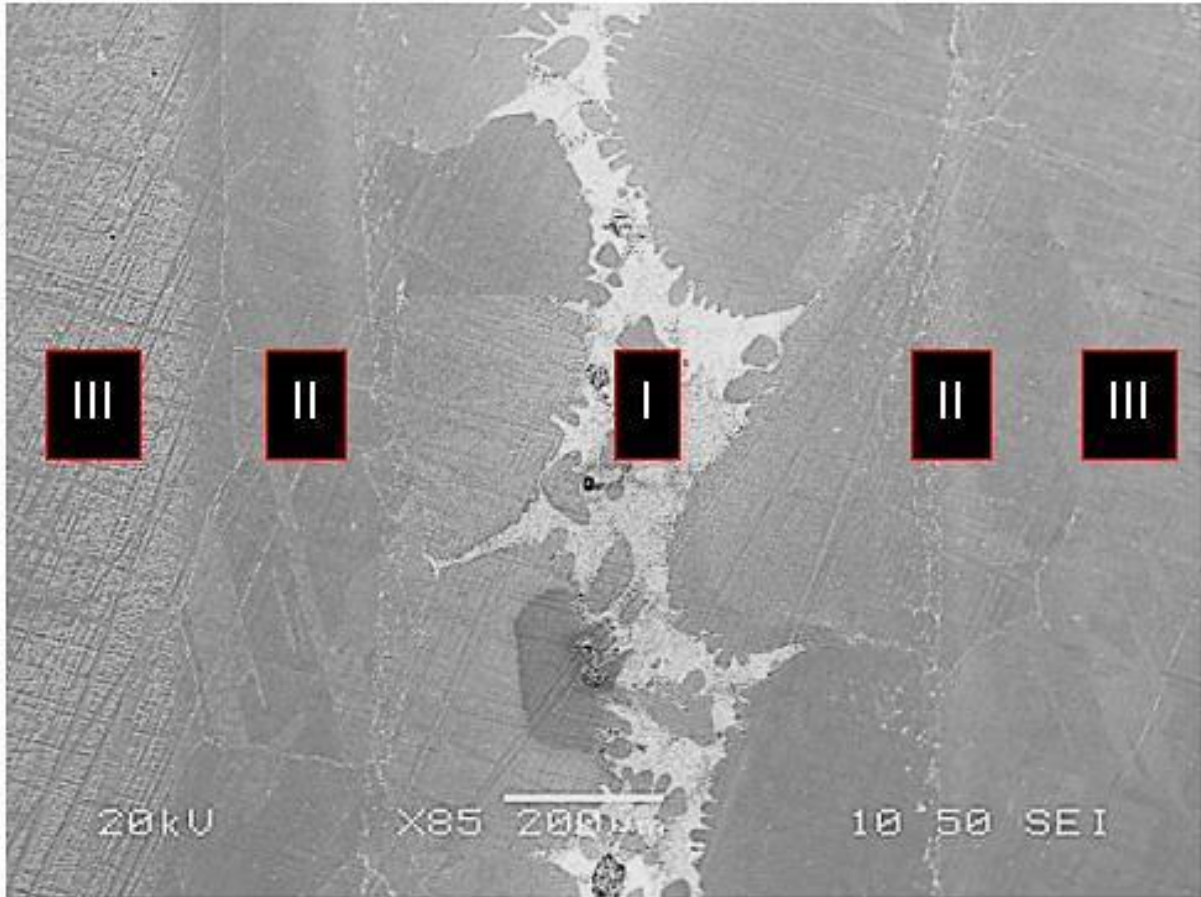


Figure 4.1: Microstructure showing the distinct regions across TLP bonded Ag/Al-Cu/Ag system

**Region II** is the isothermally solidified zone, which consists of a Ag-rich solid solution phase. This region is formed as a result of compositional changes in the liquid phase induced by the diffusion of solutes into the substrates while the sandwich structure is being held at a constant bonding temperature.

**Region III** is the silver substrate, also known as the base metal. It is a solid matrix that consumes the solutes steadily diffusing from the liquid interlayer, which drives isothermal solidification. Therefore, the completion of the bonding process is largely dependent on the interaction between the solutes and the Ag substrates.

A consistent reduction in the width of the eutectic with increase in holding time from 1 hour to 96 hours is observed. The effect of holding time on TLP bonded joint microstructure has been studied in a plethora of published works [51]–[55]. It has previously been reported that the width of the residual liquid, which forms eutectic on cooling, reduces with time as isothermal solidification progresses. The kinetics of the isothermal solidification process was reported to obey a parabolic law relationship [45], [56] where the displacement of the solid/liquid interface is proportional to the square root of time. The parabolic law is also known as the square root law, and the relationship is of the type given in equation 4.1 below.

$$Y = \phi \cdot t^n \quad 4.1$$

$$\phi = k(4 \cdot D)^n \quad 4.2$$

Where Y is the solid/liquid interface displacement,  $\phi$  is known as the interface rate constant and provides an indication of the rate of isothermal solidification, t is the holding time, n is equal to 0.5, k is related to the solidus and liquidus concentration ratio, and D is the diffusion coefficient of the solute in the solid phase.

However, in this present work, when the eutectic width at the varying holding times are plotted against the square root of time as shown in Figure 4.2, a deviation from the linear trend can be seen. This divides the process into two regimes; from the start of the process to the point where the deviation sets off is termed the first regime while the region from where deviation begins is termed the second regime.

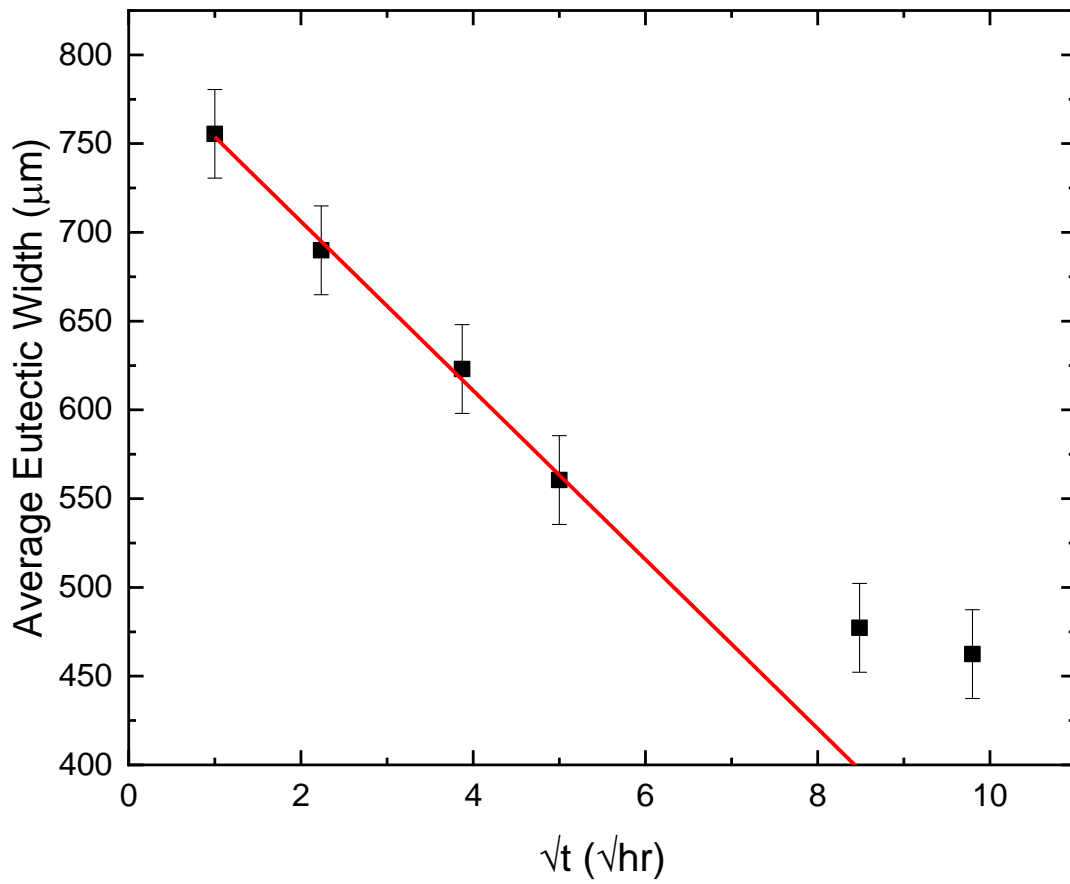


Figure 4.2: Plot of average eutectic width against square-root of time for Ag/Al-Cu/Ag samples bonded at 820°C

The deviation from linearity, which implies a deviation from the square root law has also been reported in the literature [57] but it was attributed to the presence of a second solute diffusing from the interlayer into the substrates. According to the concept of second solute, the first regime should be controlled by one solute – which is usually the faster diffusing solute – and the second regime by the second solute, which diffuses at a slower rate. As such, it is expected that in the ternary system, Ag|Al-Cu|Ag, the first regime of the process would be controlled by Cu since it has a higher diffusivity in Ag [58] and the second regime would be controlled by Al [59].

As earlier stated, for isothermal solidification to take place, there must be diffusion of solutes from the liquid interlayer through the solid/liquid interface into the substrates, and as a result, a concentration gradient of the diffusing solutes must exist. To identify the solutes diffusing in the first and second regimes, EDS analysis was carried out on all the bonded samples. The concentration profile obtained from the EDS analysis of the sample bonded for 96 hours is illustrated in Figure 4.3. The concentration profiles reveal only a concentration gradient of Cu in the first and second regimes. This suggests that the isothermal solidification process is controlled by the diffusion of one of the two MPD solutes present in the interlayer. Therefore, contrary to the concept of second solute, this finding suggests that the deviation from the square root law may be caused by a factor that is inherently related to the diffusion phenomenon of one solute diffusing in a solvent. To investigate this, a binary system where there is only one solute present in the interlayer is used.

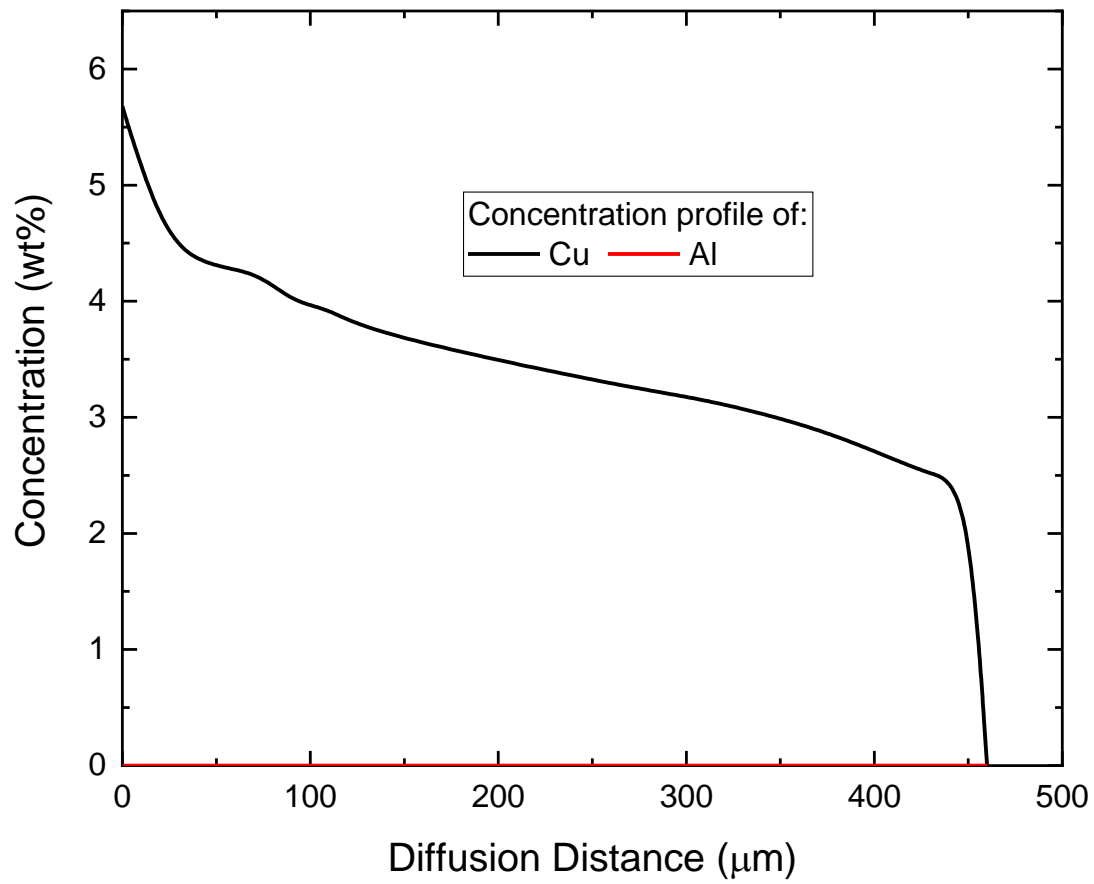


Figure 4.3: Concentration profile of Cu – with its origin starting from the solid/liquid interface – for Ag|Al-Cu|Ag sample bonded at 820°C for 96 hours

#### 4.1.2. Binary System – Ag|Cu|Ag

A different set of TLP bonding experiments are carried out using pure Ag substrates and a pure Cu interlayer foil. The samples are bonded at a temperature of 820°C. The holding times are again varied from 1 hour to 96 hours. A micrograph of one of the bonded samples showing the different regions at the joint is illustrated in Figure 4.4. It shows the typical structure of the bonded joint. The formation of a continuous centerline eutectic can be seen along the joint. The width of the eutectic was found to reduce with increase in holding time. The average eutectic widths obtained from all the bonded samples are plotted against the square root of time and is shown in Figure 4.5.

Similar to what was observed in the ternary system, a deviation from the square root law occurred during the bonding process. To further analyze this, the plots of the average eutectic widths for both ternary and binary systems were juxtaposed as shown in Figure 4.6. It is observed from the graph that the slopes of the linear curves for Ag|Al-Cu|Ag system and Ag|Cu|Ag system appear parallel in the first regime as well as in the second regime. This agrees with the suggestion that the entire isothermal solidification process is likely controlled by only one solute, which is Cu in this case. Therefore, the use of a binary system shows that the occurrence of deviation may be due to other factors, aside from a second diffusing solute.

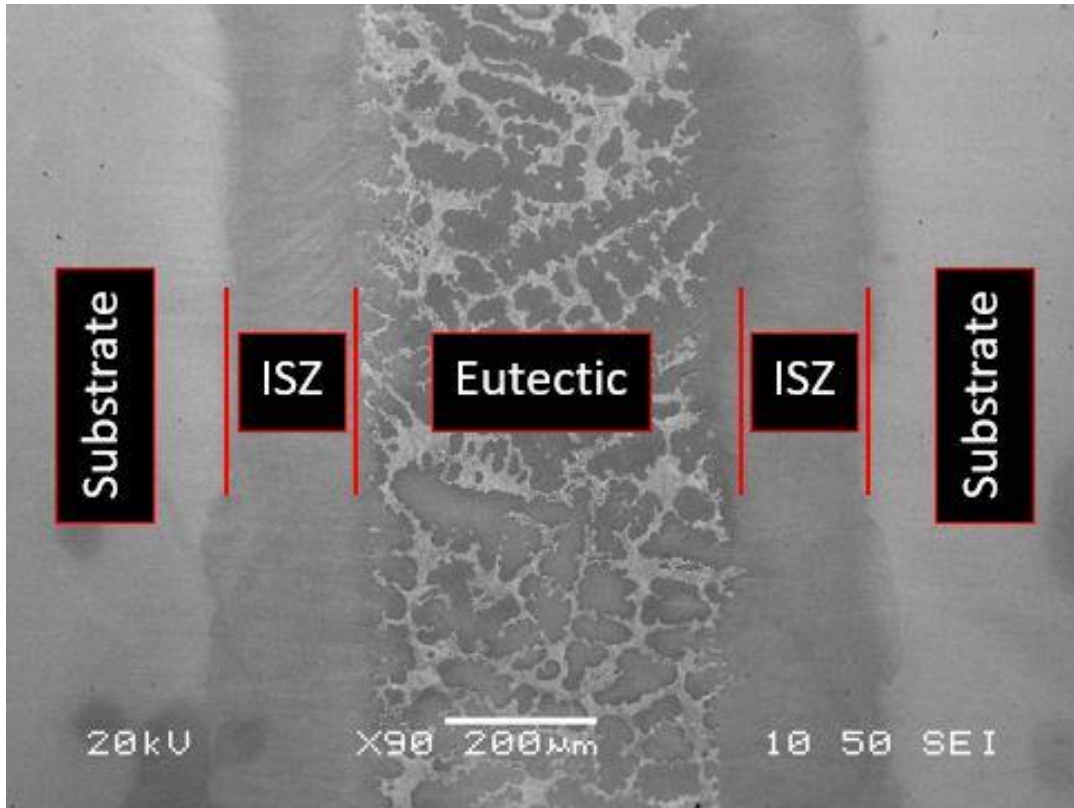


Figure 4.4: SEM micrograph showing the typical microstructure of TLP bonded Ag/Cu/Ag system

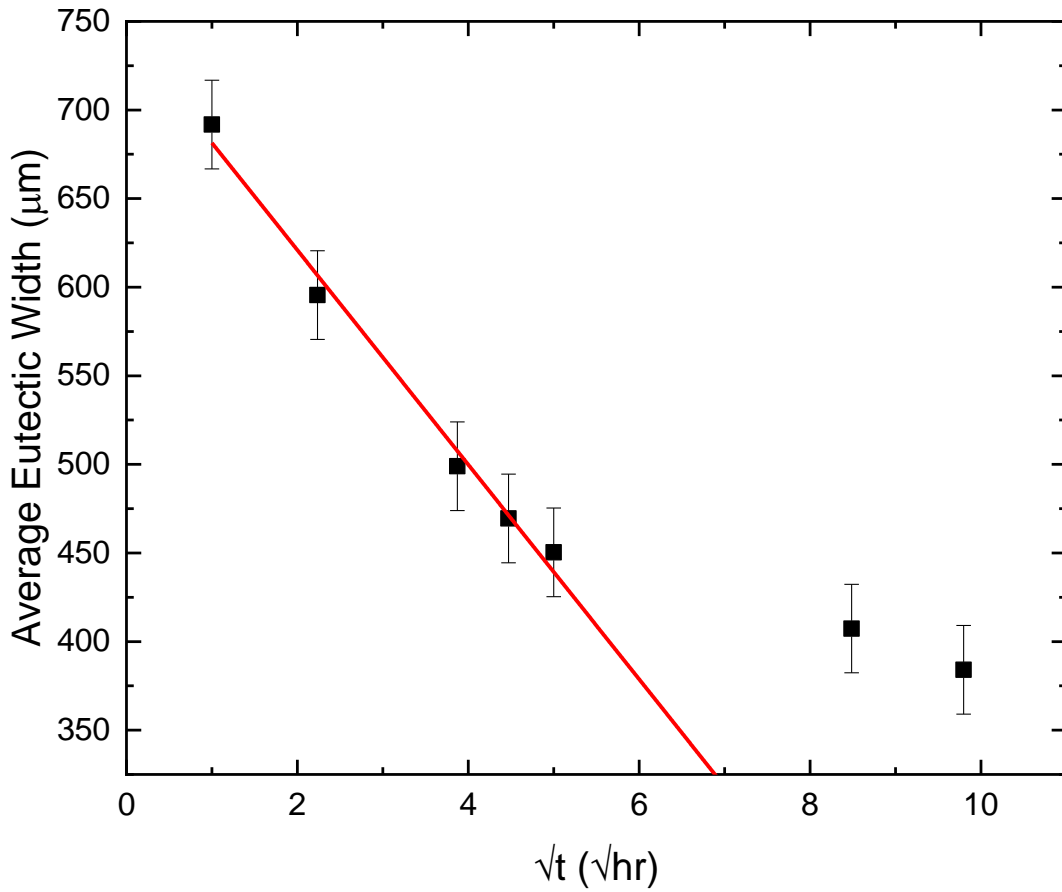


Figure 4.5: Plot of average eutectic width against square-root of time for Ag|Cu|Ag bonded at 820°C

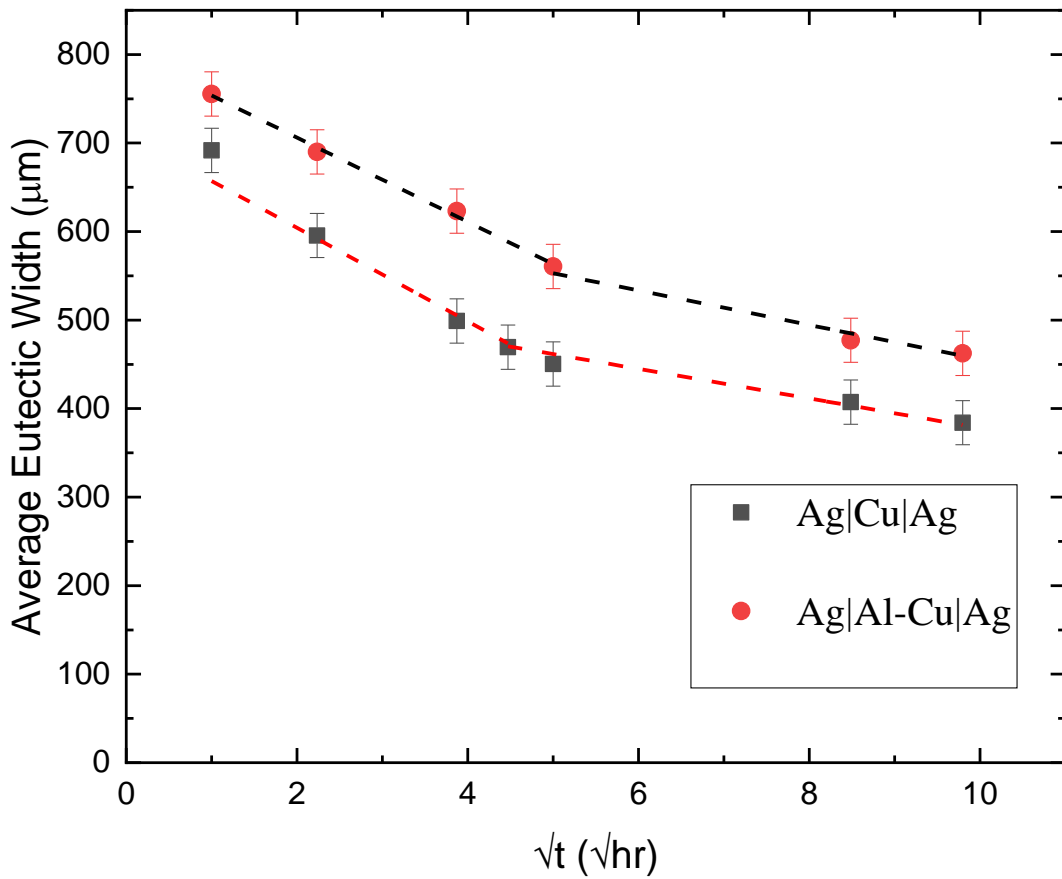


Figure 4.6: Plot of average eutectic width against square-root of time for Ag|Al-Cu|Ag and Ag|Cu|Ag

Naicheng et al. [60] studied the kinetics of the isothermal solidification stage during TLP bonding of a single-crystal superalloy using Ni-Cr-B powder interlayer. It was discovered that the isothermal solidification kinetics deviated from the parabolic law after some time during the process. Naicheng et al. [60] suggested that the deviation from the parabolic law was associated with the formation of second-phase precipitates in the substrate near the ISZ/substrate interface; the region became fully saturated with boride precipitates, which served as the sink for B, thereby completely changing the consumption velocity of B. The change in consumption velocity of B slowed down the growth rate of the ISZ, causing a deviation from the standard parabolic model. However, in the present work, B is not present in the interlayer and no second phase precipitates are observed during bonding of Ag substrates using Cu interlayer, yet deviation from the parabolic law is seen to have occurred.

It has also been suggested in the literature [61] that deviation from parabolic law is caused by grain growth in the region adjacent to the solid/liquid interface also known as the isothermally solidified zone. The study was done by J. F. Li et al. [61] on the kinetics of the interfacial reaction in Ag|Sn|Ag system during TLP bonding. In this system, instead of a solid solution phase, intermetallic composites (IMCs) were formed in the regions adjacent to the solid/liquid interface. The formation and growth of these IMCs are controlled by the diffusion of Sn solutes from the interlayer into the substrates. Therefore, the consumption rate of the solute atoms, which controls the growth kinetics of the IMCs, also known as coarsening of the IMCs, determines the rate of the isothermal solidification process. The initial stage of the process was controlled by grain boundary diffusion but as the grains of the IMCs got coarser, the process became volume-diffusion controlled, thereby, causing a deviation from the parabolic law. It was indicated that grain growth is responsible for the deviation from parabolic law.

In this present work, Ag|Cu|Ag samples were bonded at 790°C, 820°C and 850°C to study the grain sizes during isothermal solidification. It is observed from the chart in Figure 4.7, which shows the plot of the average eutectic width against the square root of time, that a deviation from the square root law occurred at the three bonding temperatures. An SEM examination of the bonded samples was conducted; the microstructure of the samples, shown in Figure 4.8 reveals that the grain sizes before and after deviation are comparable. This indicates that grain growth is likely not responsible for the deviation. Moreover, it was reported in the literature [60] that deviation from the square root law occurred during TLP bonding of a single-crystal superalloy. Therefore, based on the results of this current work, it seems that deviation from parabolic law is likely related to the fundamental diffusion phenomenon of a solute in a matrix.

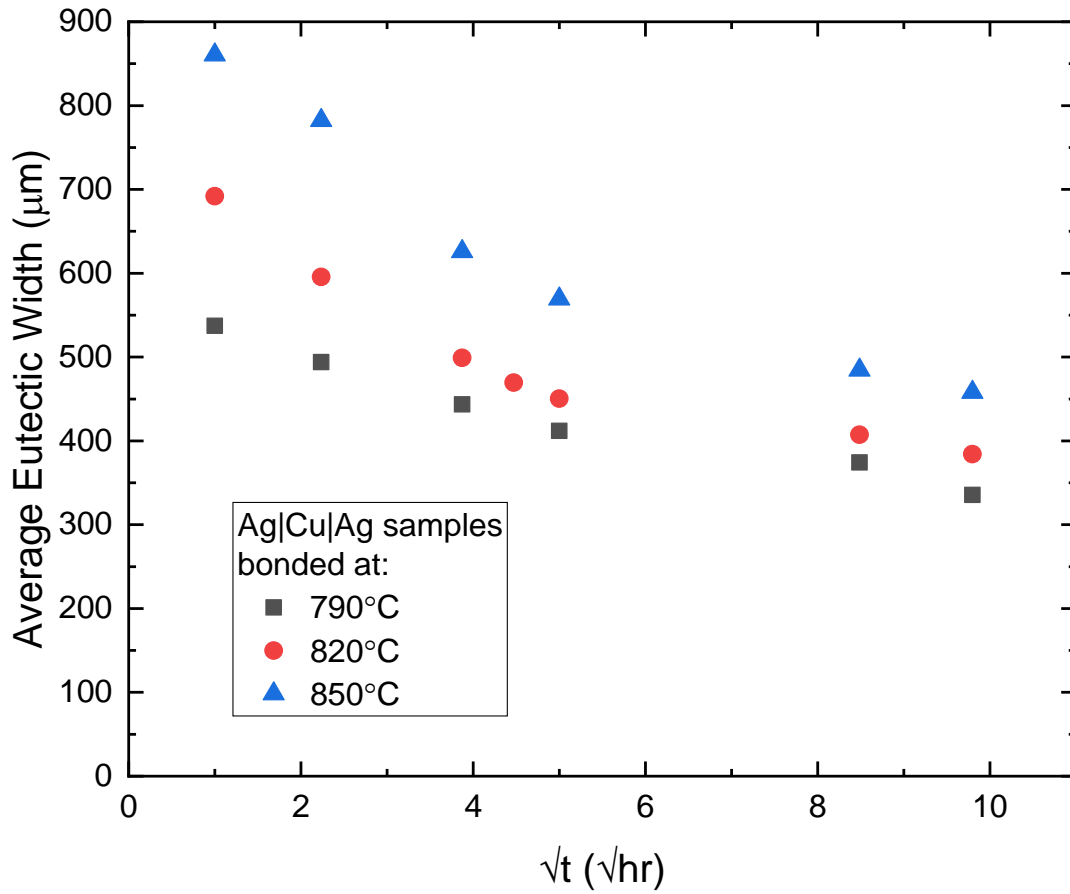


Figure 4.7: Plot of average eutectic width against square-root of time for Ag|Cu|Ag at temperatures of 790°C, 820°C, and 850°C

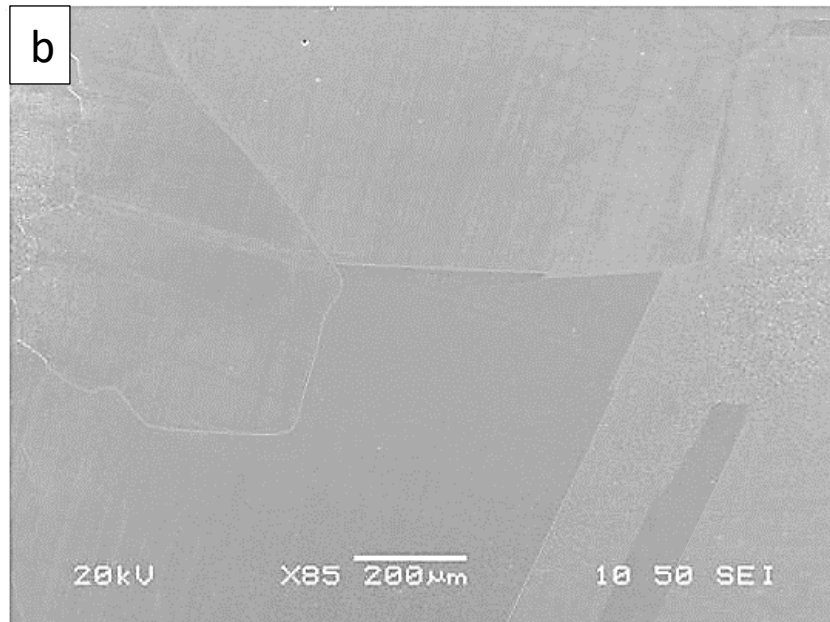
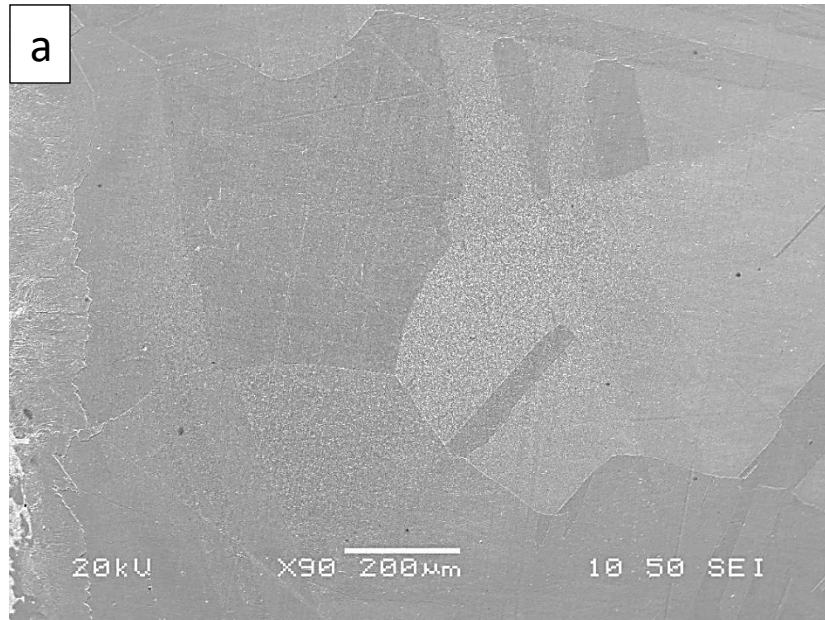


Figure 4.8: (a) 1 hour and (b) 96 hours SEM micrographs showing the grains in the region adjacent to the solid/liquid interface for Ag|Cu|Ag samples bonded at 850°C

The term *deviation* implies that there is a change in the slope of the linear plot of the solid/liquid interface displacement against the square root of time. It is important to note that the term  $\phi$  in Equation 4.1, which is the slope of the linear plot, is a function of the diffusion coefficient  $\mathbf{D}$  as seen in Equation 4.2. Hence, the slope of the line is affected by the diffusion coefficient. In most TLP bonding models, i.e. the standard diffusion models of TLP bonding found in the literature, diffusion coefficient  $\mathbf{D}$  is usually assumed to be constant. This is a trivial assumption and can be consequential.

In reality, the diffusion coefficient  $\mathbf{D}$  can vary. This means that diffusion coefficient can change throughout the entire TLP bonding process instead of maintaining a constant diffusion coefficient. It has been suggested in the literature [62] that diffusion coefficient can be given by,

$$D_{\text{var}} = D_t D_c \quad 4.3$$

Where  $D_t$  is the time-dependent diffusion coefficient i.e.  $D = f(t)$ , and  $D_c$  is the concentration-dependent diffusion coefficient i.e.  $D = f(C)$ .

$\mathbf{D}_t$  could be due to the structural changes occurring in the metals during TLP bonding process [63]. As time progresses during the process, Cu solutes from the liquid interlayer consistently diffuses into the bulk Ag substrates; structural changes occur along the diffusion path that could cause strain and eventually, generate dislocations, thereby, changing the diffusion coefficient.

$\mathbf{D}_c$  is due to compositional changes along the diffusion path. As the concentration of the diffusing solute is changing with distance, the diffusion coefficient may also change.

Understanding that  $D$  can have a dynamic nature since it can be sensitive to structure and compositional changes, it is logical that the diffusion coefficient,  $D$ , during isothermal solidification may be influenced by time and solute concentration. If  $D$  is variable, it is expected that the relationship between the displacement of the solid/liquid interface and the square root of holding time will deviate from linearity at some point during the process. Qualitatively, the dependence of  $D$  on concentration and holding time can be examined by studying the concentration profiles of the bonded samples. A diffusion coefficient varying with concentration will produce a concentration profile that has a very sharp front [64]. In this study, the effect of concentration on the  $D$ , which is termed  $D_c$ , can be observed experimentally from the EDS analysis carried out on the Ag|Cu|Ag samples bonded at 790°C, 820°C, and 850°C. Figure 4.9 to Figure 4.11 show the concentration profiles of the samples bonded for holding times varying from 1 hour to 96 hours. The *sharp front* observed from the graph is a strong indication that the  $D$  is not constant but changing with concentration.

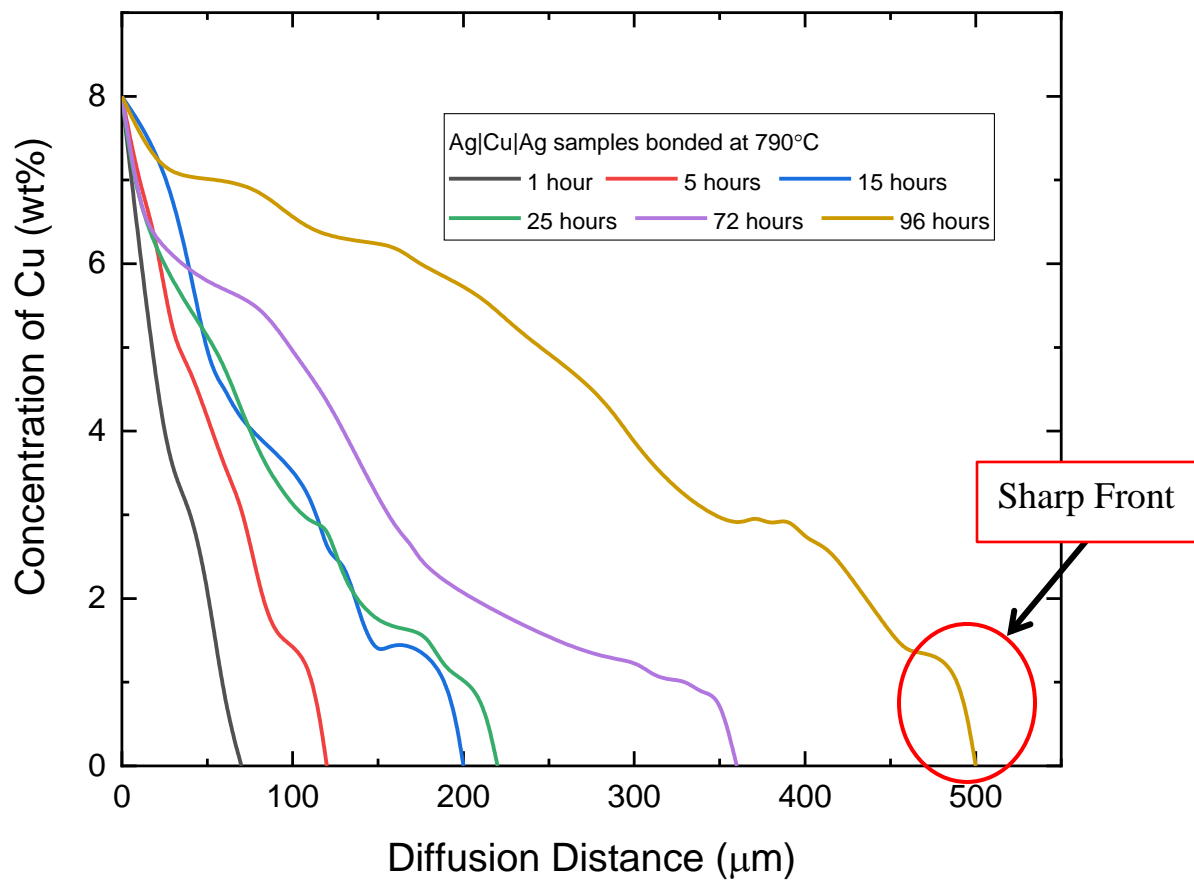


Figure 4.9: Concentration profile of Cu – with its origin starting from the solid/liquid interface – for Ag|Cu|Ag samples bonded at 790°C and held for times ranging from 1 hour to 96 hours

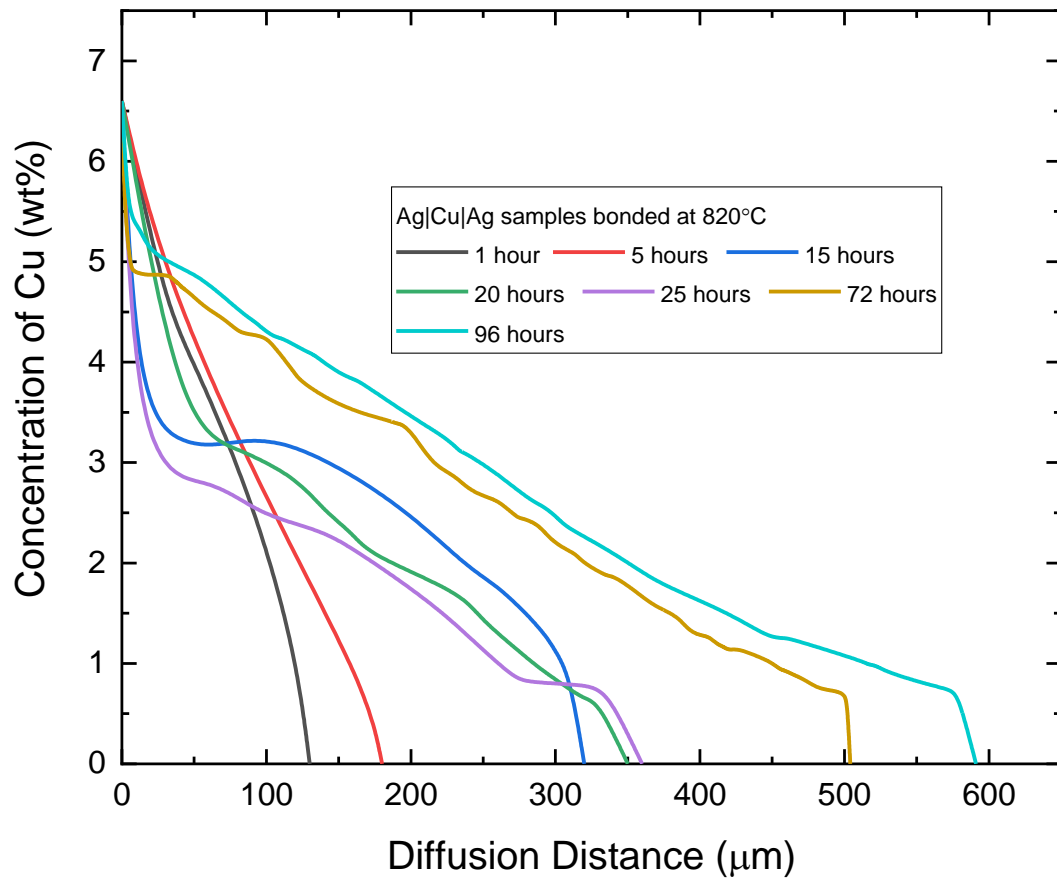


Figure 4.10: Concentration profile of Cu – with its origin starting from the solid/liquid interface – for Ag|Cu|Ag samples bonded at 820°C and held for times ranging from 1 hour to 96 hours

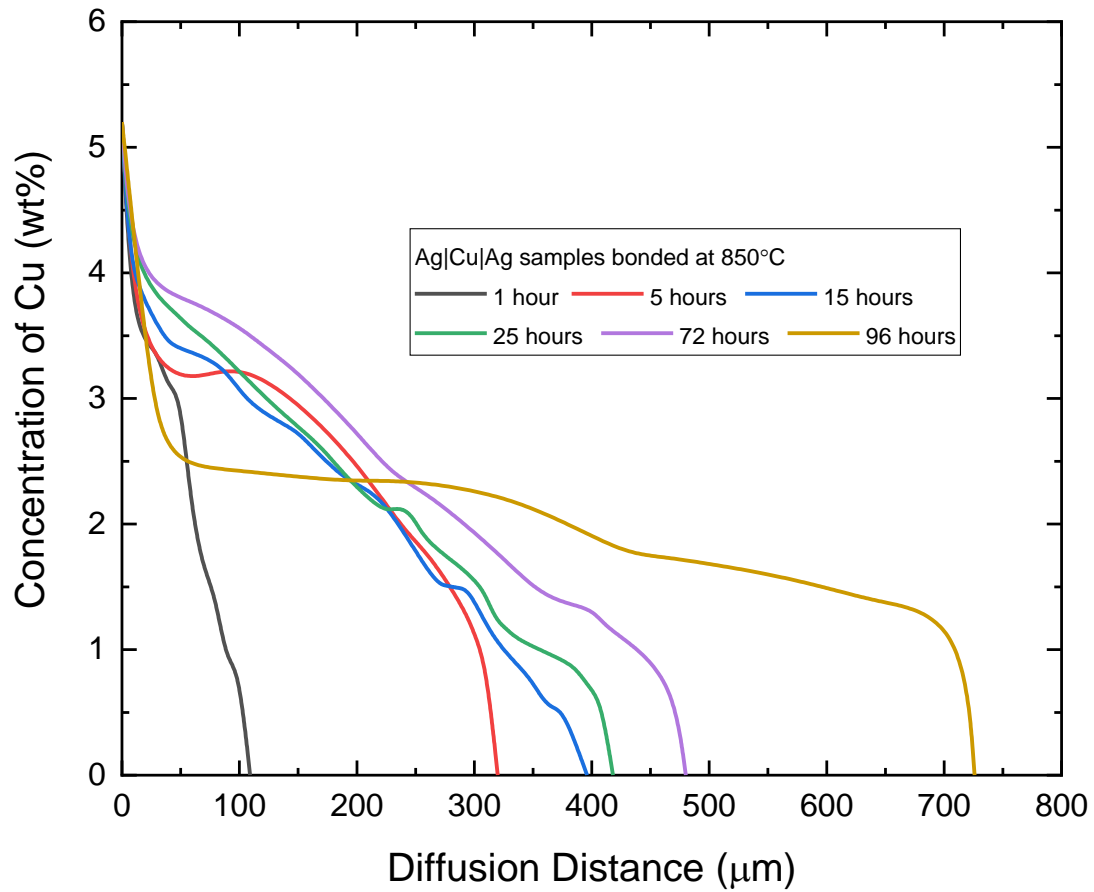


Figure 4.11: Concentration profile of Cu – with its origin starting from the solid/liquid interface – for Ag|Cu|Ag samples bonded at 850°C and held for times ranging from 1 hour to 96 hours

To examine the influence of time on the dependence of the diffusion coefficient on concentration,  $D_t$ , three conditions are considered: firstly, if the diffusion coefficient as a function of concentration is not changing with time, the concentration profile is expected to retain a consistent shape at any given time. Secondly, a constant concentration-dependent diffusion coefficient means that the function of the diffusion curve remains unchanged with time, therefore, the concentration profiles should be continuous – and not intersect – with increase in holding time. The chart in figure 4.12 provides a schematic of the expected trend of the concentration profiles if  $D_c$  is constant with time. Lastly, if the concentration-dependent diffusion coefficient is independent of time, the concentration profiles for the different holding times, at a fixed temperature, is expected to coincide on the x-axis when plotted against a normalized diffusion distance, which is the diffusion distance by the square root of time [65].

In this present work, the concentration profiles of the samples bonded at temperatures of 790°C, 820°C, and 850°C were examined for the conditions stated above. It is clearly seen from the concentration profiles in Figure 4.9 to Figure 4.11 that the shape of the diffusion curve, at a fixed temperature, changes as the holding time is increased from 1 hour to 96 hours. Also, it is observed that the curves intersect each other, which means that the function of the diffusion curve is changing with time, and thus, the diffusion coefficient changes. Furthermore, the concentration profiles obtained for the various holding times, at temperatures of 790°C, 820°C, and 850°C are plotted as a function of a normalized diffusion distance in Figure 4.13 to Figure 4.15. The experimental error range for the normalized diffusion distance was found to be between  $\pm 5 \mu\text{m}$ . It is seen from the plots that the concentration profiles, at a fixed temperature, for the different holding times do not coincide. Therefore, these results qualitatively show that the diffusion coefficient is a function of concentration and time.

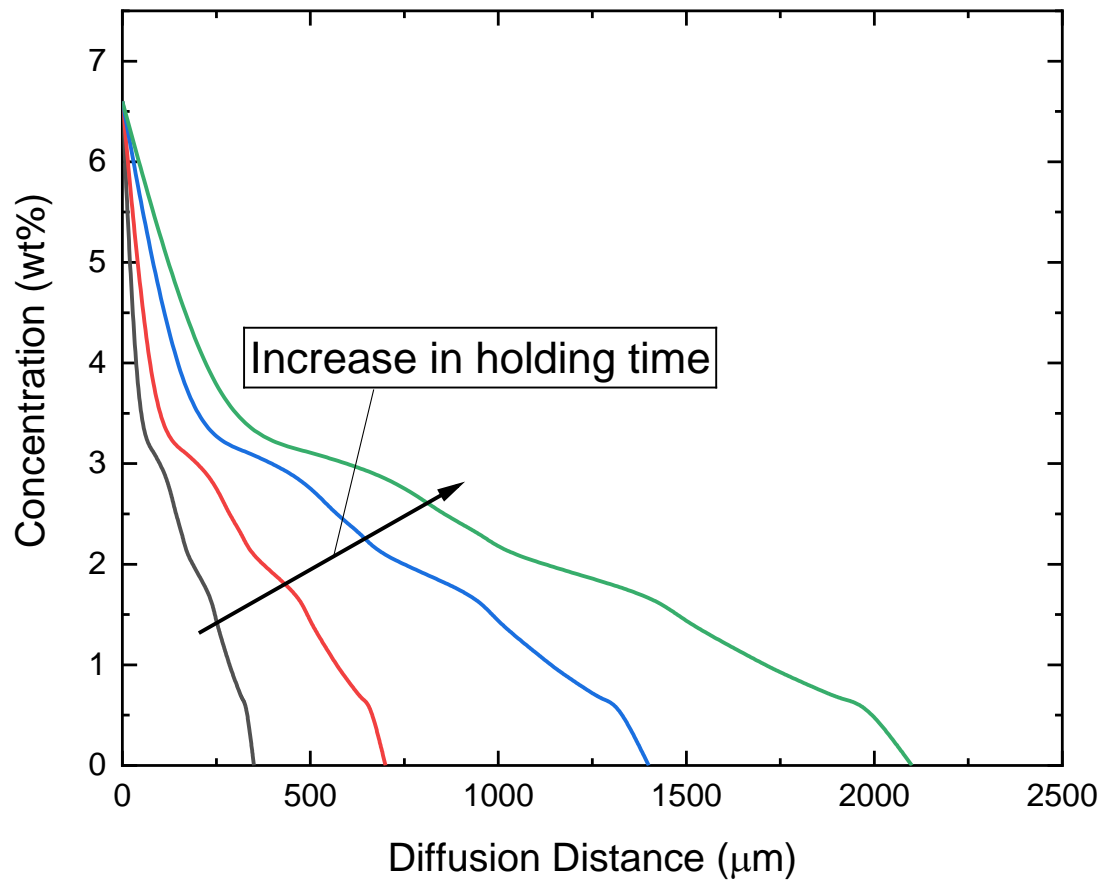


Figure 4.12: Expected trend of the concentration profiles when  $D=f(C)$  is not changing with time

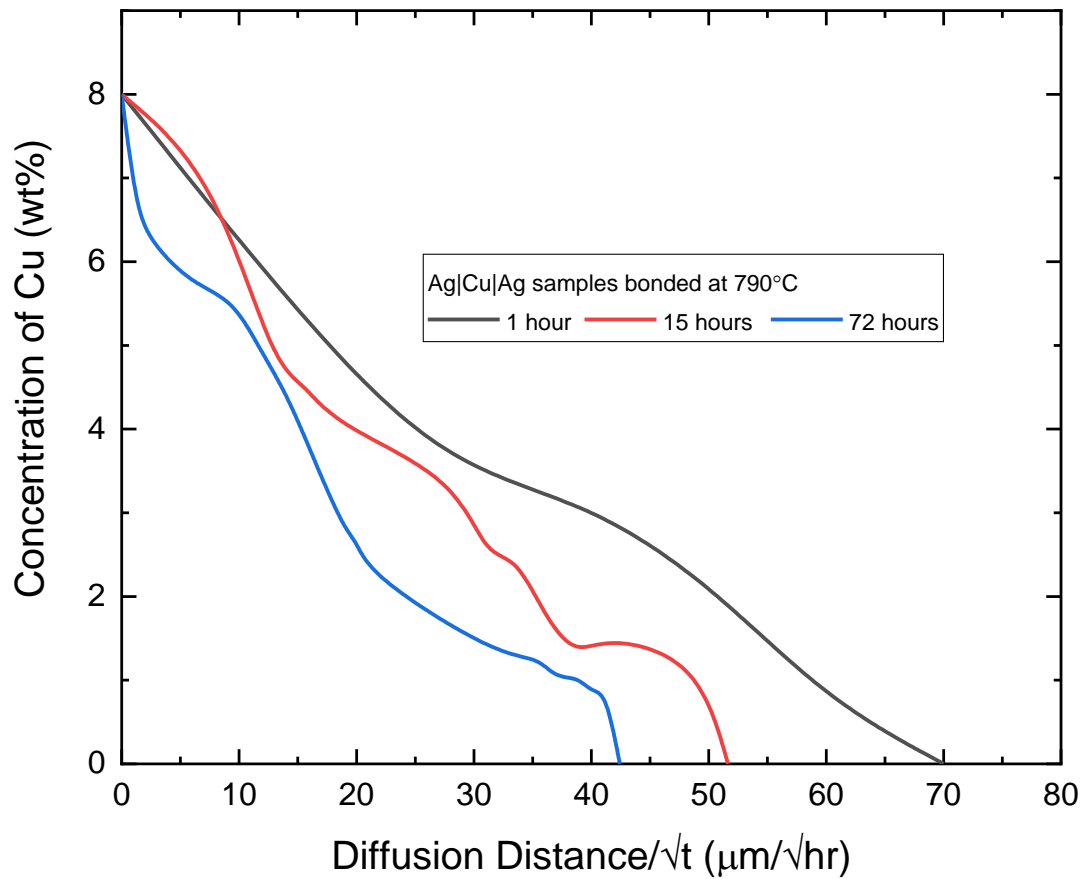


Figure 4.13: Concentration profile of Cu plotted on a normalized x-axis for Ag|Cu|Ag samples bonded at 790°C and held for times ranging from 1 hour to 96 hours

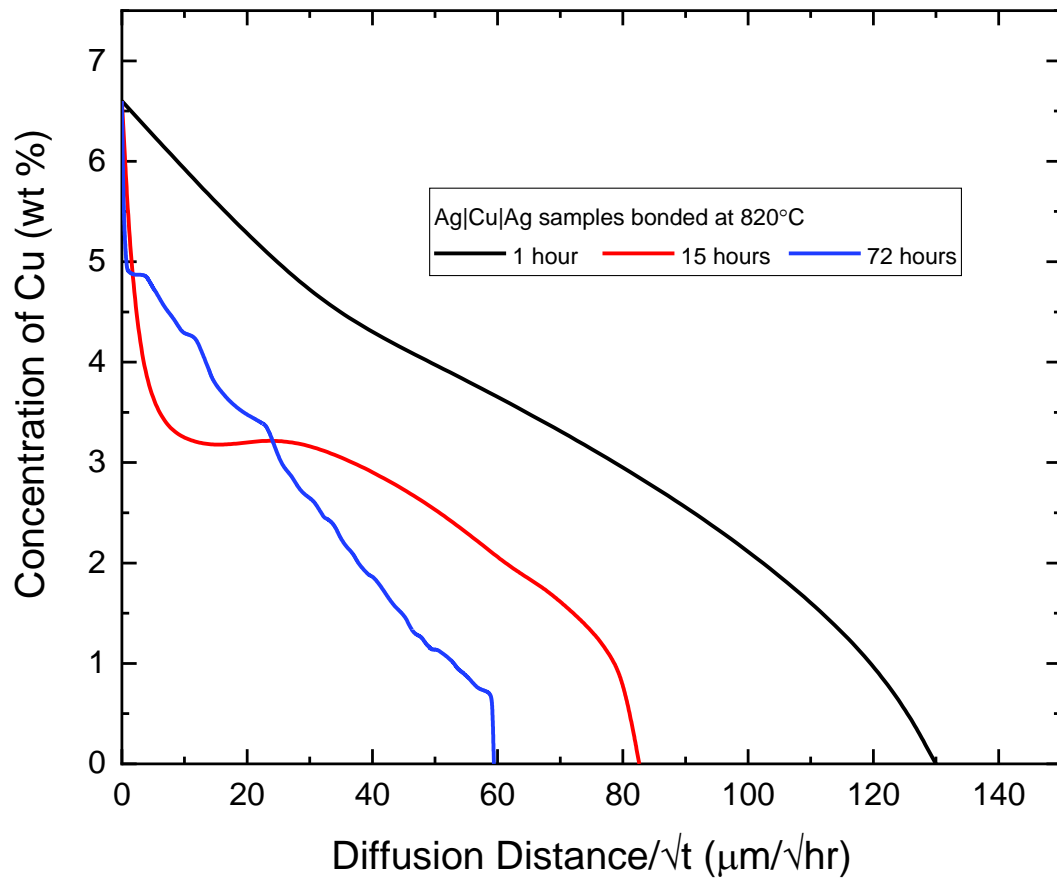


Figure 4.14: Concentration profile of Cu plotted on a normalized x-axis for Ag|Cu|Ag samples bonded at 820°C and held for times ranging from 1 hour to 96 hours

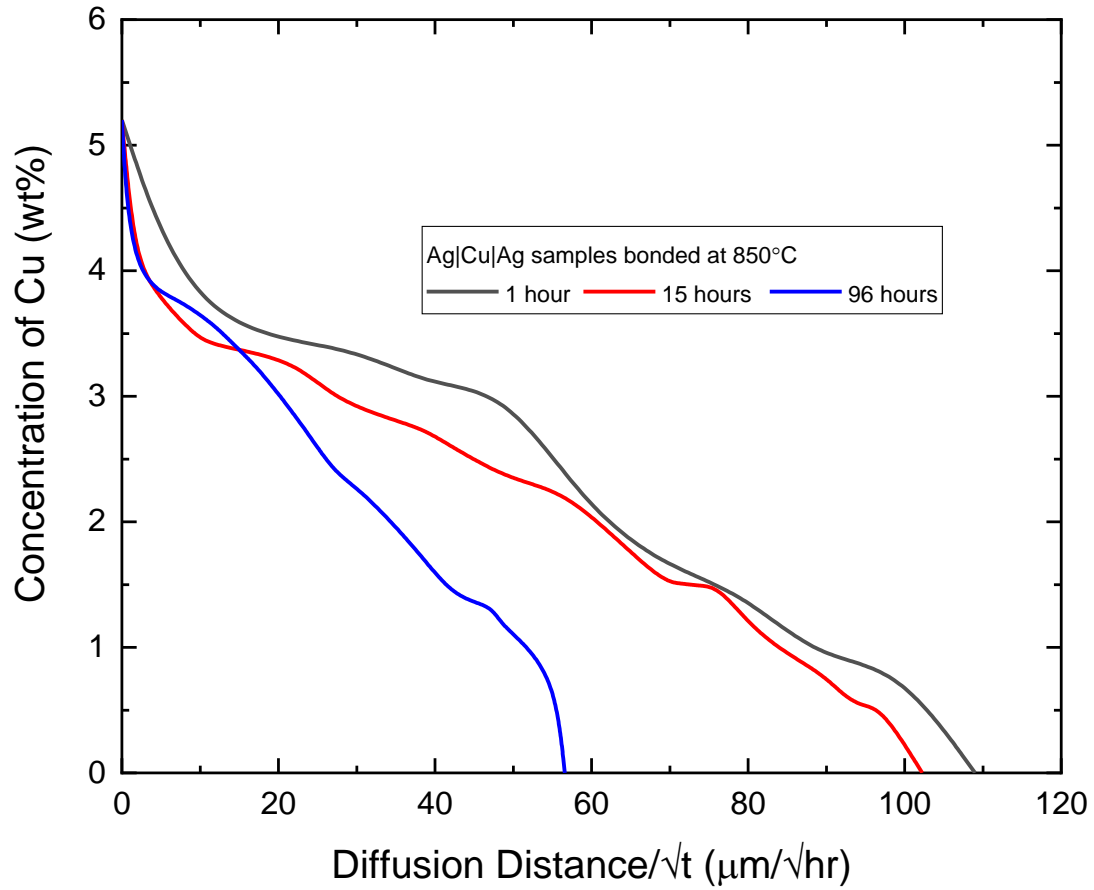


Figure 4.15: Concentration profile of Cu plotted on a normalized x-axis for Ag|Cu|Ag samples bonded at 850°C and held for times ranging from 1 hour to 96 hours

### 4.1.3. Quantitative Evaluation of Variable Diffusion Coefficient Using Hall's Method

A quantitative analysis of the concentration profiles of the Ag|Cu|Ag samples bonded at temperatures of 790°C, 820°C, and 850°C is presented in this section. The aim is to validate the observations made in the preceding section, where **D** is qualitatively found to be varying with concentration and time. Hall's method is selected as the preferred method for calculating the diffusion coefficient because it yields reliable results at low concentrations of the solute [66], which is the situation in this present work.

At a given time, the probability plot of the concentration distribution in Figure 4.13 to Figure 4.15 will yield a straight line as illustrated in Figure 4.16 below. The slope and intercept of the line is used to calculate the diffusion coefficient. The equation of the straight line is given as:

$$\frac{c}{c_0} = \text{erf}(c(h\lambda + k)) \quad 4.4$$

$$u = (h\lambda + k) \quad 4.5$$

Where  $\frac{c}{c_0}$  the concentration ratio,  $c$  is the concentration of Cu,  $\lambda$  is the diffusion distance divided by the square root of time,  $h$  and  $k$  are, respectively, the slope and intercept of the line.

Therefore, from equation 4.4 and 4.5,

$$\frac{c}{c_0} = \text{erf}(cu) \quad 4.6$$

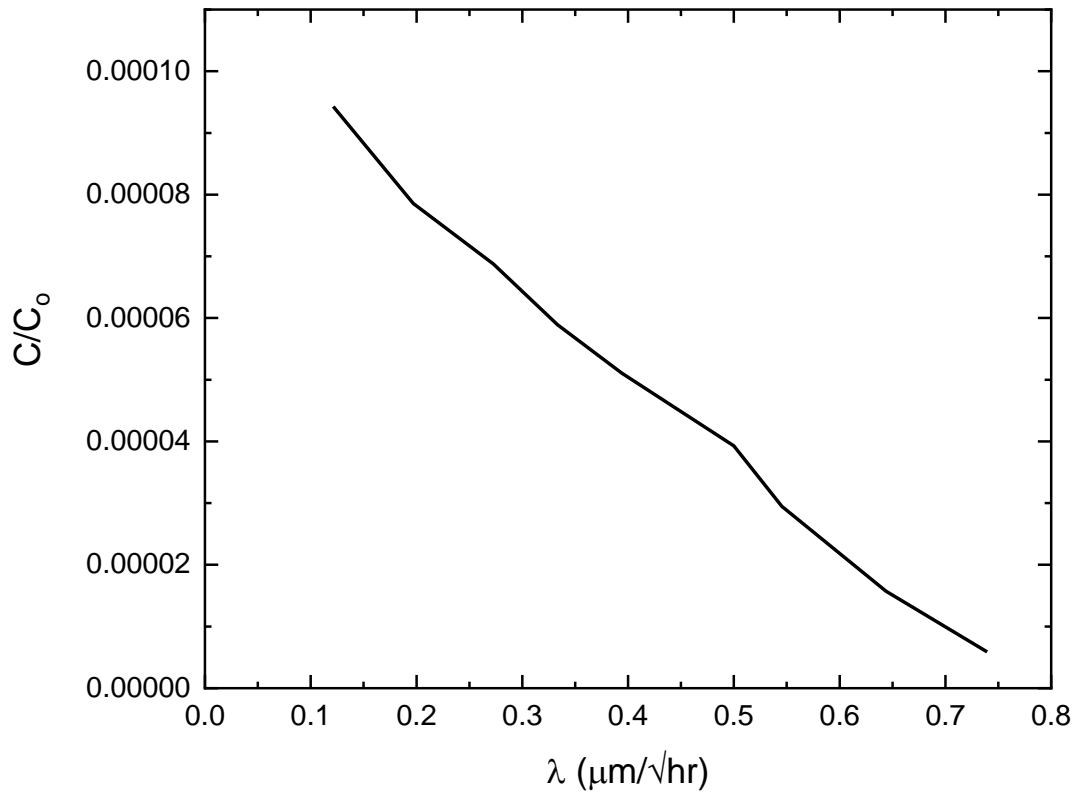


Figure 4.16: Probability plot of  $c/c_0$  against  $\lambda$  for Ag/Cu/Ag at 820°C

The concentration ratio written in terms of the cumulative standard normal density function is:

$$\frac{c}{c_0} = \frac{1}{2}(1 + \text{erf}(u)) \quad 4.7$$

$$u = \text{erf}^{-1}\left(2\frac{c}{c_0} - 1\right) \quad 4.8$$

Using the values of  $u$ ,  $h$  and  $k$  obtained from the probability plots, the concentration-dependent diffusion coefficient is computed as [66]:

$$D(c) = \frac{1}{4h^2} + \frac{k\sqrt{\pi}}{2h^2} \exp(u^2) \frac{c}{c_0} \quad 4.9$$

In this work, the concentration-dependent diffusion coefficient is calculated for different holding times to show the variation of  $\mathbf{D}$  with concentration and time. Figure 4.17 to Figure 4.19 shows the plot of the diffusion coefficients against concentration for holding times of 1 hour, 15 hours, and 72 hours. It is seen from the plots that the diffusion coefficient increases with concentration but reduces with time. The results of this analysis confirm that  $\mathbf{D}$  is not constant but varies with concentration and time.

In conclusion, if  $\mathbf{D}$  is a function of concentration and time as indicated by the experimental results obtained in this study, the slope of the solid/liquid interface displacement plotted against the square root of time, termed as  $\Phi$  and defined by equation 4.2, would change, since it is a function of  $\mathbf{D}$ . Therefore, it is expected that as consequence, a deviation from the square root law will occur during the isothermal solidification process. In contrast to the idea of the deviation from the parabolic law being attributed to the presence of a second diffusing solute, second phase precipitate or grain growth, this work shows that the deviation from the parabolic law during isothermal solidification can be explained by a variable diffusion coefficient that changes with concentration and time.

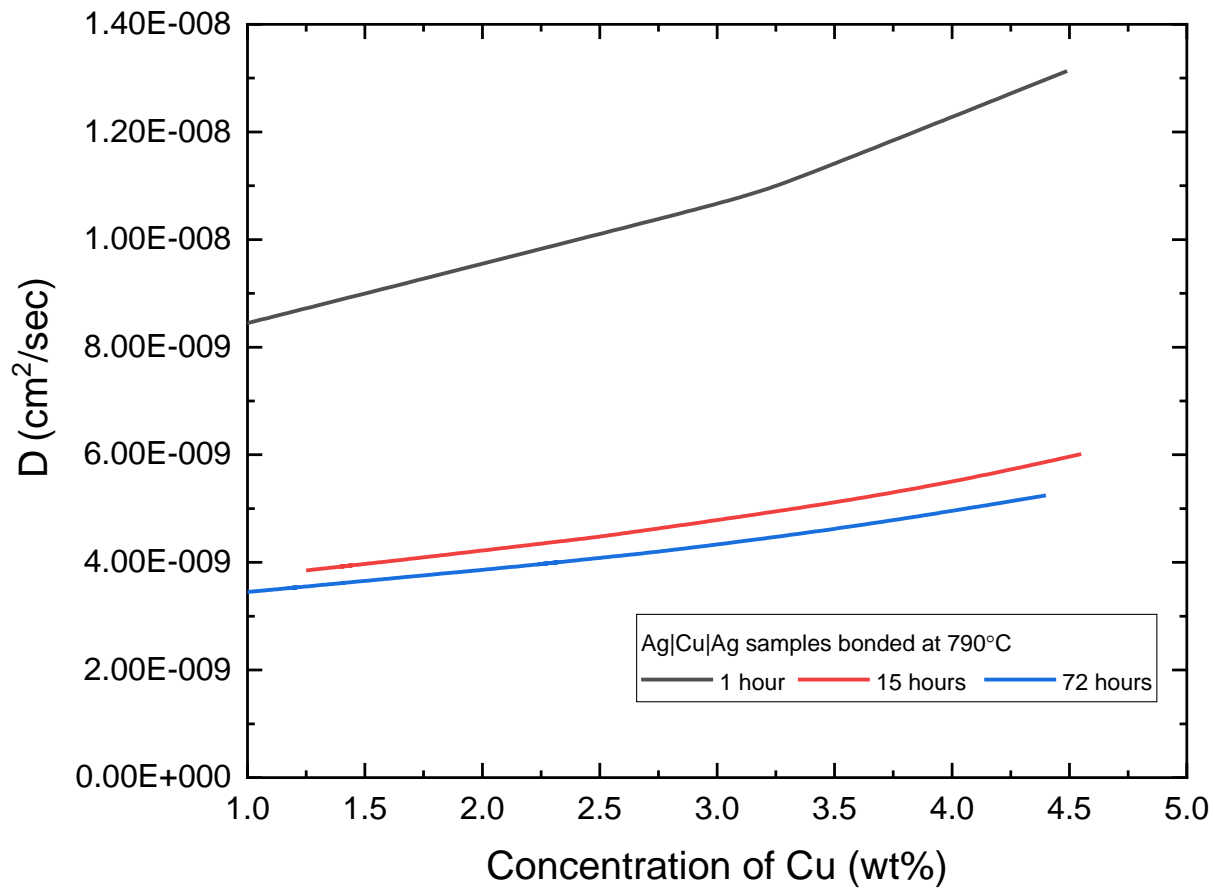


Figure 4.17: Plot of diffusion coefficient against concentration at 790°C for 1 hour, 15 hours, and 72 hours

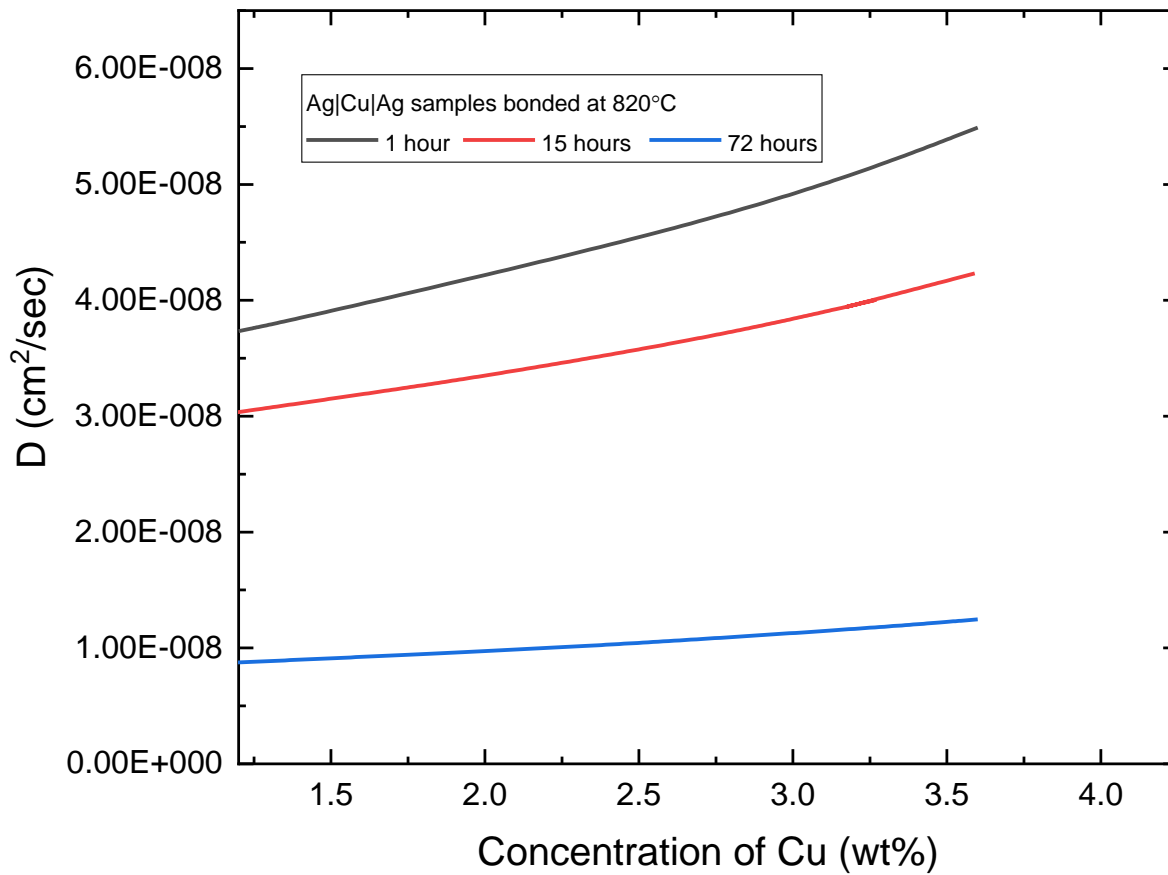


Figure 4.18: Plot of diffusion coefficient against concentration at 820°C for 1 hour, 15 hours, and 72 hours

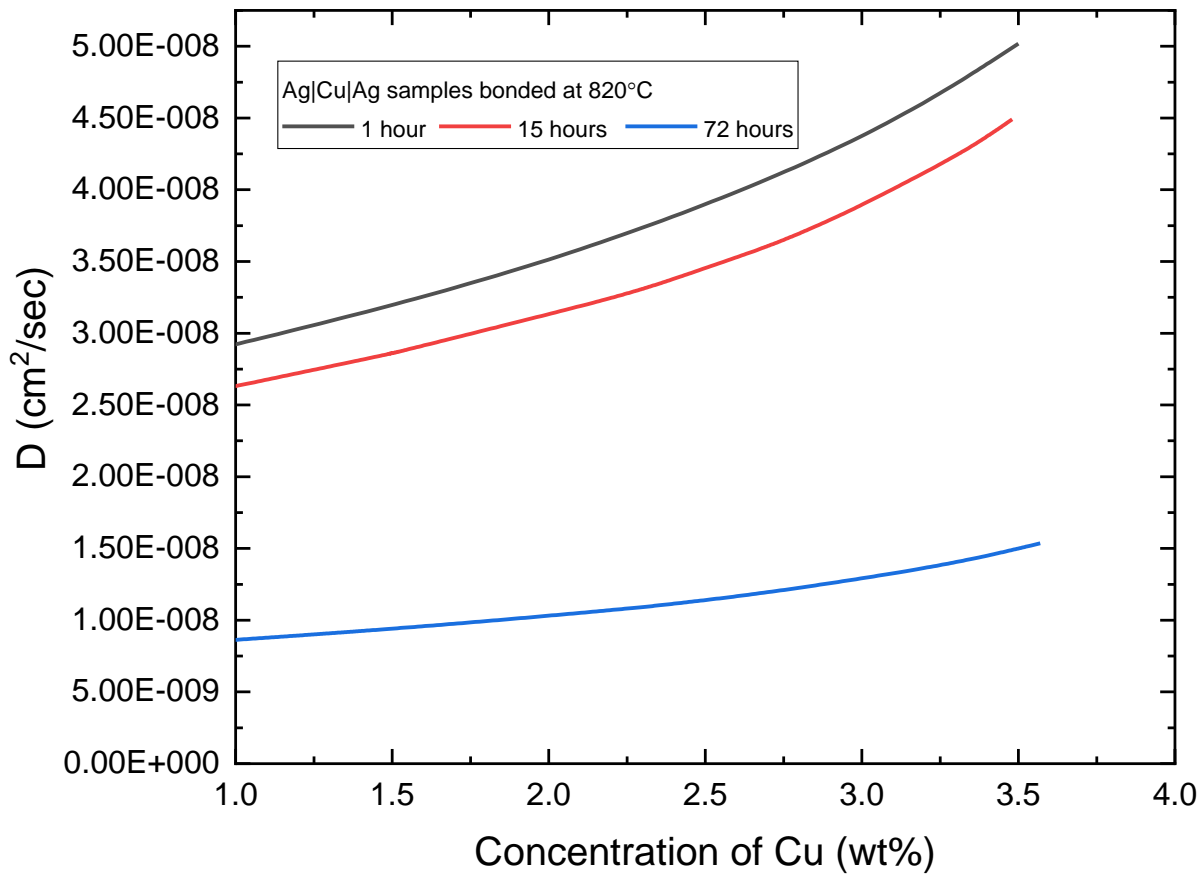


Figure 4.19: Plot of diffusion coefficient against concentration at 850°C for 1 hour, 15 hours, and 72 hours

## 4.2. Effect of bonding temperature on the kinetics of TLP bonding process

Temperature is an important factor that affects the kinetics of isothermal solidification during TLP bonding; the kinetics of isothermal solidification is controlled by the extent of penetration of the solutes into the substrates, which is strongly influenced by the bonding temperature. The depths of penetration of Cu into the substrates at different holding times are plotted against temperature and shown in Figure 4.20. The chart shows that the depth of penetration of Cu into the substrates increases as the bonding temperature is increased from 790°C to 850°C. An increase in the depth of penetration of Cu means that the rate of diffusion of Cu from the liquid interlayer is faster with increase in temperature. It was stated earlier in section 4.1 that the rate of isothermal solidification is directly controlled by the rate of diffusion of Cu into the substrates, therefore, the increase in the depth of penetration of Cu with increase in the bonding temperature implies that the rate of isothermal solidification – denoted as  $\phi$  in equation 4.2 – increases as temperature is increased.

It can be expected that, for a given holding time, an increase in the rate of isothermal solidification would produce a smaller amount of residual liquid that forms eutectic when cooled to room temperature [67], [68]. However, contrary to this expectation, it is observed from Figure 4.7 that the width of the residual liquid increases as the bonding temperature is increased. This apparent contrast in behavior can be attributed to the increase in the volume of the liquid phase when the bonding temperature is increased. It can be seen from the phase diagram in Figure 2.3 that the liquidus concentration of Cu reduces as temperature is increased, therefore, leading to increased dissolution of the substrates and a subsequent widening of liquid zone to attain the equilibrium liquid composition. Therefore, it is possible that the increase in the volume of the

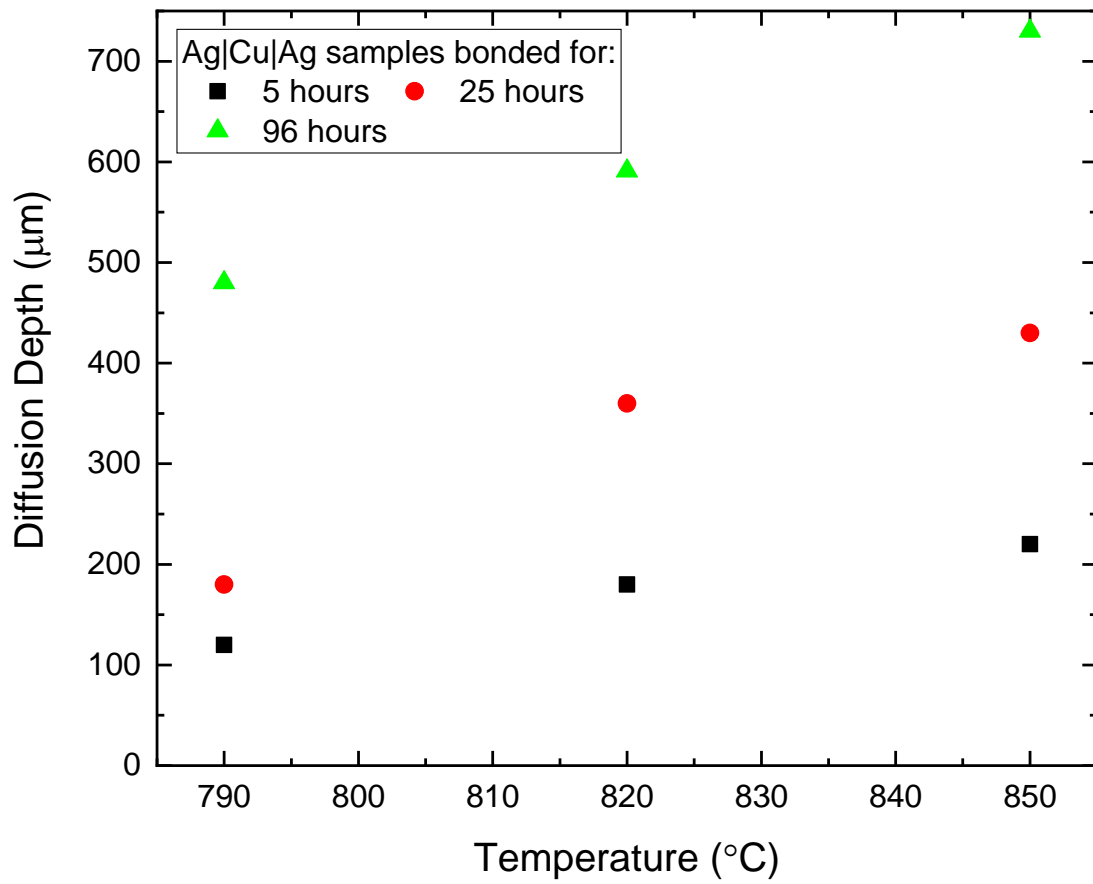


Figure 4.20: Plot of diffusion depth against the bonding temperature

liquid phase nullified the increase in the rate of isothermal solidification, thereby, leading to a situation where the eutectic increases with increase in temperature. Nevertheless, this may not be the case in all TLP bonding systems.

If an increase in the volume of the liquid with increase in temperature can nullify the effect of the increase in the rate of isothermal solidification, at any given time more eutectic will form at a higher temperature. This occurrence will result in a situation whereby the time required to achieve complete isothermal solidification will be prolonged with increase in temperature, despite the increase in the rate of isothermal solidification. To investigate the possibility of this behavior in Ag|Cu|Ag system, assuming that the diffusion coefficient is constant, the following calculations are carried out:

$\phi$  is calculated using equation 4.3. The diffusion coefficient is calculated by Arrhenius relation:

$$D = D_o \exp\left(-\frac{Q}{RT}\right) \quad 4.10$$

Where  $D_o$  is the pre-exponential factor,  $Q$  is the activation energy for diffusion of Cu in Ag,  $R$  is the gas constant, and  $T$  is the bonding temperature.

$k$  is solved numerically using the relation [69]:

$$\frac{k(1+\operatorname{erf}(k))\sqrt{\pi}}{\exp(-k^2)} = \frac{C_{\alpha L} - C_M}{C_{L\alpha} - C_{\alpha L}} \quad 4.11$$

Where  $C_{\alpha L}$  is the concentration of Cu in the solid phase,  $C_M$  is the initial solute concentration in the substrate, and  $C_{L\alpha}$  the concentration of Cu in the liquid phase.

The pre-exponential factor and activation energy used to solve for  $D$  were obtained from the literature [70]. The concentrations  $C_{\alpha L}$ ,  $C_{L\alpha}$ , and  $C_M$  are obtained from the phase diagram in Figure 2.3. The dependence of  $\phi$  on the bonding temperature is graphically represented in Figure 4.21.

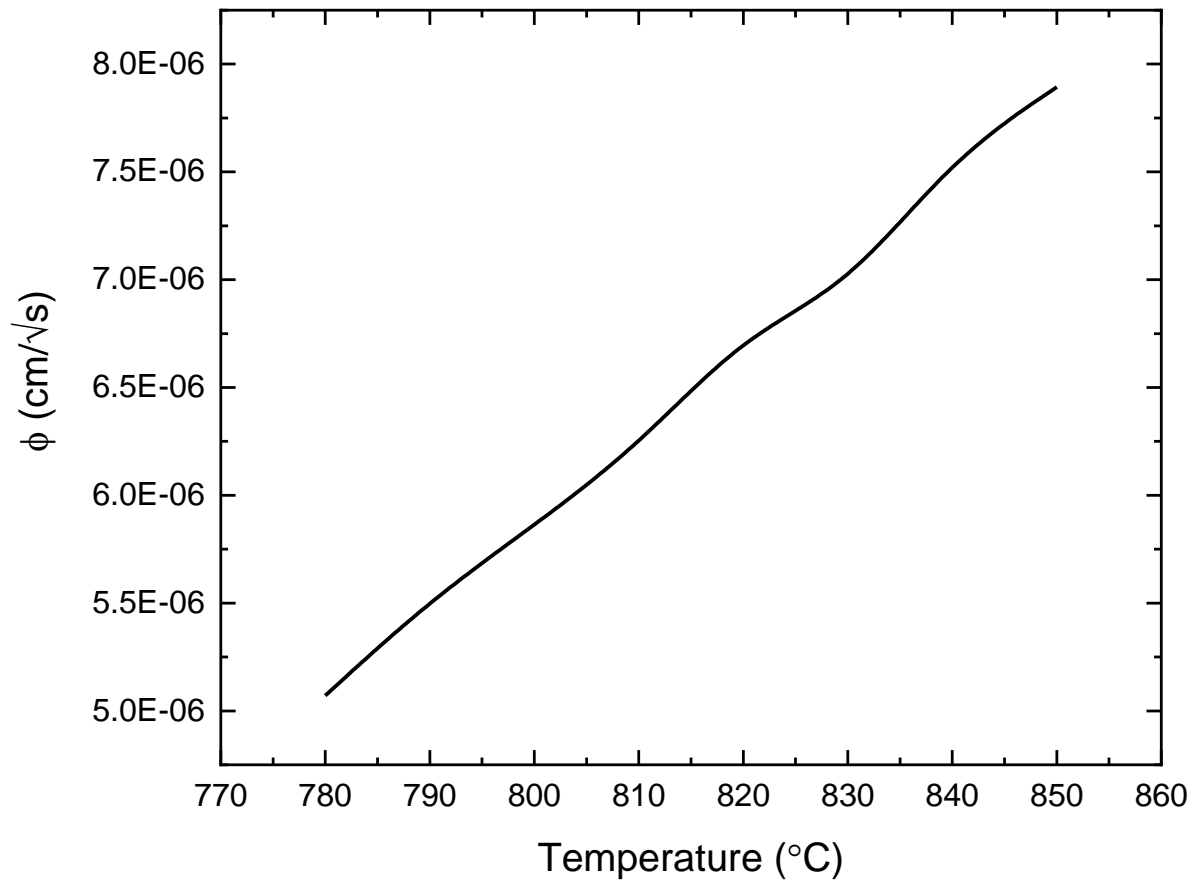


Figure 4.21: Plot of rate of isothermal solidification against temperature

The chart shows that  $\phi$  increases as temperature is increased, which is in agreement with the experimental observations in this study. The maximum width of the liquid phase formed at the joint can be calculated using the mass balance relation [45]:

$$W_{\max} = W_o \left( \frac{C_F}{C_{L\alpha}} \right) \quad 4.12$$

Where  $W_o$  is the initial width of the interlayer,  $C_F$  and  $C_{L\alpha}$  are the initial concentration of Cu in the interlayer and the concentration of Cu in the liquid phase, respectively.

The maximum liquid widths obtained using Equation 4.12 are plotted against temperature in Figure 4.22. It is observed from the chart that the maximum width of the liquid increases with temperature, and it increases by 1.8 orders of magnitude when the bonding temperature is increased from 790°C to 850°C. Further calculations were done to check the effect of the increase in  $W_{\max}$  and  $\phi$  on the time required to achieve complete isothermal solidification of the liquid phase, given by the relation [69].

$$t_f = \frac{W_{\max}^2}{16k^2D} \quad 4.13$$

The time required to achieve complete isothermal solidification is plotted against temperature in Figure 4.23 and the plot shows that despite the increase in  $\phi$  with increase in temperature, the time required to completely use up the liquid is prolonged. This is attributable to the increase in the volume of the liquid in the joint with increase in temperature. Therefore, it is found that in Ag|Cu|Ag system, the potential benefit of the increase in the rate of isothermal solidification can be nullified by the increase in the volume of the liquid at the joint with increase in temperature during TLP bonding. This in effect can cause an extension in the time required to achieve complete isothermal solidification when temperature is increased.

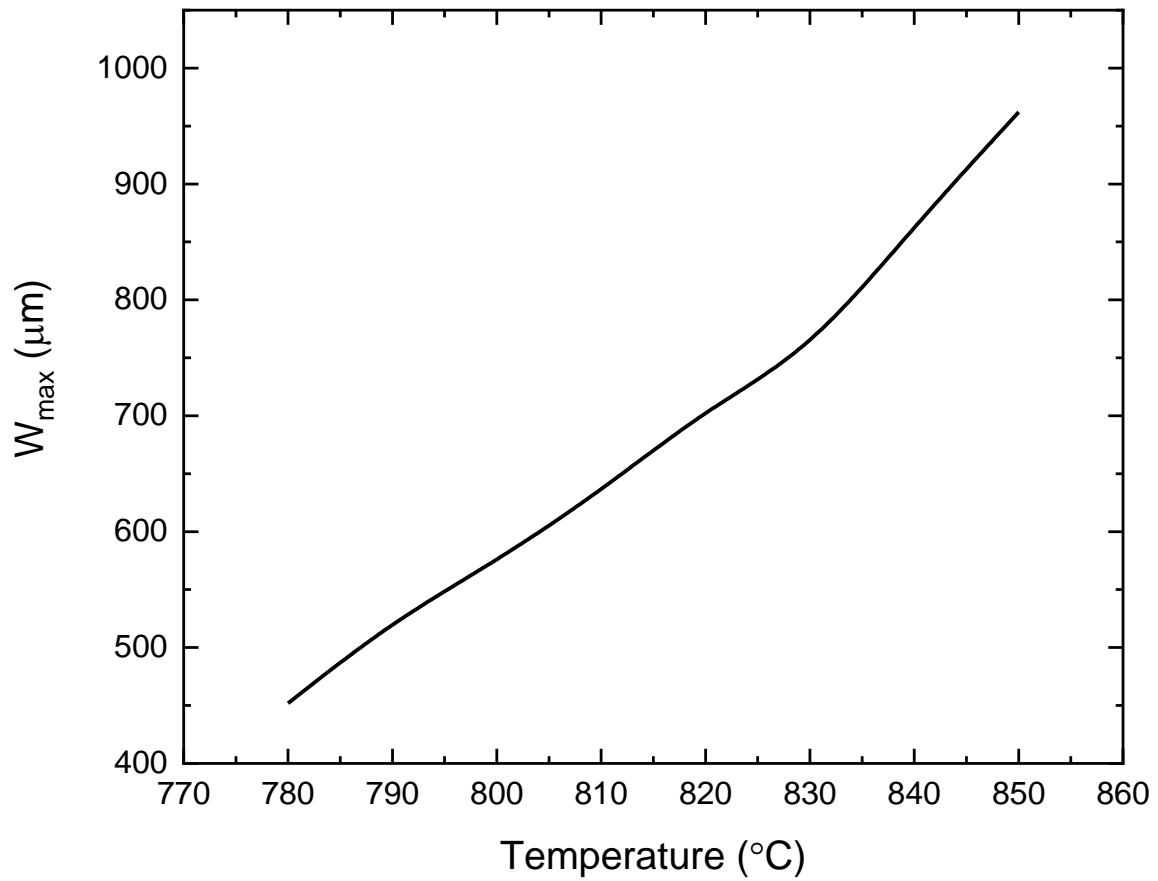


*Figure 4.22: Plot of maximum width of liquid against temperature*

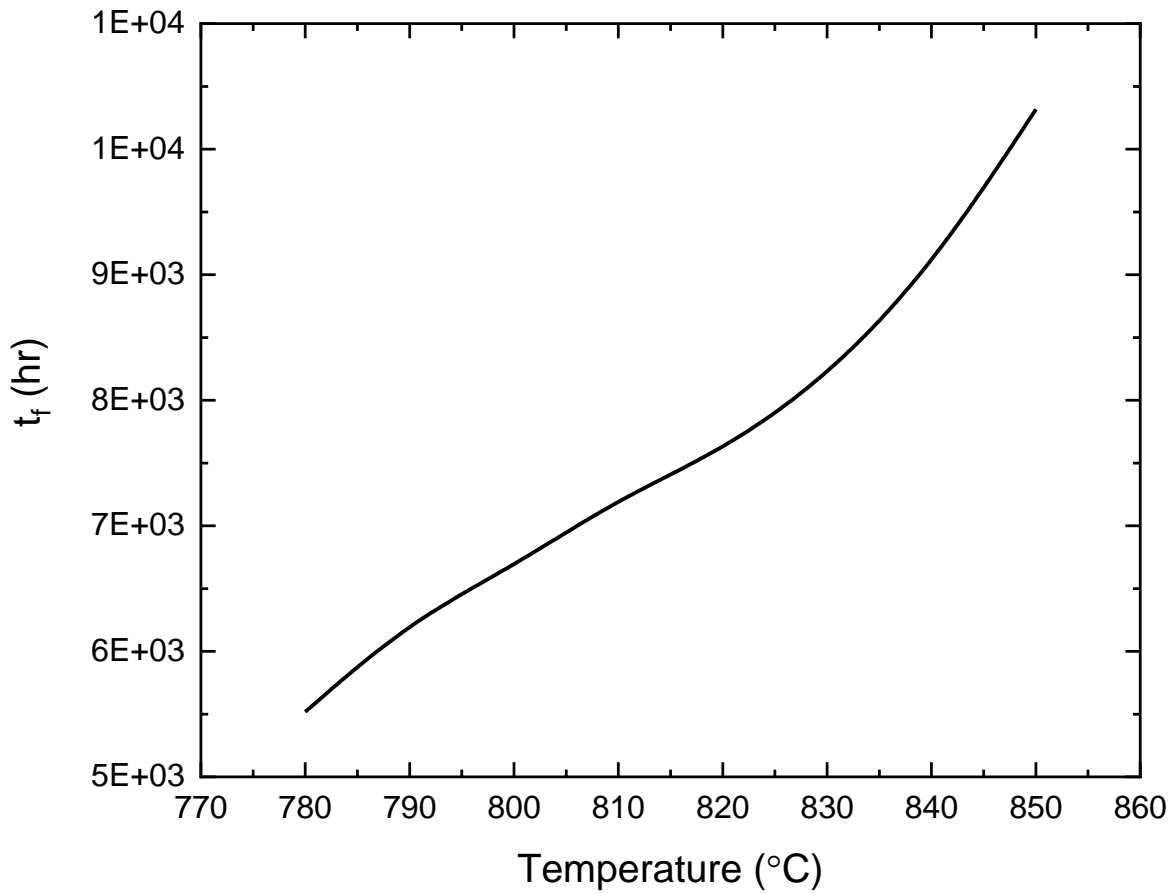


Figure 4.23: Plot of time required for complete isothermal solidification against temperature

## 5. CONCLUSIONS AND SUGGESTIONS FOR FUTURE WORK

### 5.1. Conclusions

An analysis of the kinetics of Transient Liquid Phase bonding was successfully carried out using Ag|Al-Cu|Ag ternary system and Ag|Cu|Ag binary system. The conclusions drawn from the results obtained are summarized below.

1. Microstructural analysis of the TLP bonded joints for both the ternary and binary systems show the formation of continuous centerline eutectic. The size of the eutectic was found to reduce as holding time was increased.
2. In contrast to standard TLP bonding models where the kinetics of isothermal solidification follows a parabolic rate law, the results obtained show a deviation from the parabolic rate law.
3. This study shows that a deviation from the parabolic law can occur without the presence of a second solute. Cu was observed to be controlling the isothermal solidification process in the ternary system despite the presence of a second solute in the interlayer; the only concentration gradient existing in the isothermally solidified zone and the substrate after the TLP bonding experiments was that of Cu, a concentration gradient of Al was absent. Additionally, deviation also occurred during TLP bonding of the binary system where there was only one solute present in the interlayer.
4. Deviation from parabolic law can occur without the formation of second phase precipitates. No second phase precipitates were observed in the systems used. Cu has

substantial solubility in Ag; therefore, the chance of forming second phase precipitates was eliminated.

5. Grain growth had been suggested to be the factor responsible for the deviation from the parabolic law during isothermal solidification, however, microstructural characterization of TLP bonded Ag|Cu|Ag samples reveal similar grain sizes at shorter and longer bonding times.
6. In contrast to a constant diffusion coefficient generally assumed in the literature, analysis of the experimental concentration profiles by the use of Hall's method shows that diffusion coefficient changes with concentration and time. This key experimental finding has not been previously reported during TLP bonding in the literature.
7. The variation of the diffusion coefficient with concentration and time during the isothermal solidification process can explain the deviation from the parabolic law.
8. An increase in bonding temperature from 790°C to 850°C resulted in an increase in the size of the residual liquid at the joint, but nonetheless, it was found that the rate of isothermal solidification of the liquid increased as temperature was increased. This seemingly contrasting behavior is attributable to the increase in the volume of the liquid zone in the joint when temperature is increased.
9. Theoretical calculations confirm that, in Ag|Cu|Ag system, the potential benefit of the increase in the rate of isothermal solidification can be nullified by a concurrent increase in the volume of the liquid phase at higher temperatures.
10. Therefore, in contrast to what is generally assumed (i.e. reduction in  $t_f$  with increase in temperature), the results of this study show that an increase in the rate of isothermal

solidification with increase in temperature does not necessarily mean that the time,  $t_f$ , required to eliminate the deleterious eutectic microconstituent through complete isothermal solidification will be shorter.

## **5.2. Suggestions for Future Work**

1. Supplementary study on the effect of variable diffusion coefficient should be carried out with other binary systems.
2. Numerical analysis and experimental investigations should be conducted to study the occurrence and effect of a variable diffusion coefficient in ternary and higher order systems, and to what extent the findings from this research work extend to these systems.

## REFERENCES

- [1] FAA, "Aircraft Metal Structural Repair," *Aviat. Maint. Tech. Handbook—Airframe Vol. 1*, 2012.
- [2] S. W. S. Doebling, C. R. C. Farrar, M. B. M. Prime, and D. W. D. Shevitz, "Damage identification and health monitoring of structural and mechanical systems from changes in their vibration characteristics: a literature review," *Los Alamos Natl. Lab.*, p. 133p, 1996.
- [3] S. Sharma, "No Title," *Quora*, 2017. [Online]. Available: <https://www.quora.com/What-is-fusion-welding#>.
- [4] M. Alam, "Importance and Basic Concept of Welding."
- [5] T. Debroy and S. A. David, "Physical processes in fusion welding," *Rev. Mod. Phys.*, vol. 67, no. 1, pp. 85–112, 1995.
- [6] J. ROBERTW. MESSLER, *Principles of Welding*. 1999.
- [7] K. I. Mori, N. Bay, L. Fratini, F. Micari, and A. E. Tekkaya, "Joining by plastic deformation," *CIRP Ann. - Manuf. Technol.*, vol. 62, no. 2, pp. 673–694, 2013.
- [8] G. Bussu and P. E. Irving, "The role of residual stress and heat affected zone properties on fatigue crack propagation in friction stir welded 2024-T351 aluminium joints," *Int. J. Fatigue*, vol. 25, no. 1, pp. 77–88, 2002.
- [9] J. Norrish, *Advanced welding processes*. 2006.
- [10] M. Schwartz, *Brazing*. 2003.
- [11] "Brazing - Google Search." [Online]. Available: <https://en.wikipedia.org/wiki/Brazing>. [Accessed: 17-Sep-2018].
- [12] S. Metco, "An Introduction to Brazing Fundamentals , Materials , Processing," no. 3, pp. 10–24, 2011.
- [13] O. W. Paulonis D, Duvall D, "Diffusion Bonding Utilizing. Transient Liquid Phase," no. 54, p. 3,678,570, 1971.
- [14] N. Wikstrom, O. Ojo, M. C.-S. and E. A, and undefined 2006, "Influence of process parameters on microstructure of transient liquid phase bonded Inconel 738LC superalloy with Amdry DF-3 interlayer," *Elsevier*.
- [15] H. Assadi, A. Shirzadi, E. W.-A. materialia, and undefined 2001, "Transient liquid phase diffusion bonding under a temperature gradient: modelling of the interface morphology," *Elsevier*.
- [16] O. Idowu, N. Richards, M. C.-S. and E. A, and undefined 2005, "Effect of bonding temperature on isothermal solidification rate during transient liquid phase bonding of Inconel 738LC superalloy," *Elsevier*.
- [17] N. Bosco, F. Z.-A. Materialia, and undefined 2004, "Critical interlayer thickness for transient liquid phase bonding in the Cu–Sn system," *Elsevier*.

- [18] R. Bakhtiari, A. E.-M. & Design, and undefined 2012, “The effect of gap size on the microstructure and mechanical properties of the transient liquid phase bonded FSX-414 superalloy,” *Elsevier*.
- [19] E. Norouzi, M. Atapour, M. Shamanian, and A. Allafchian, “Effect of bonding temperature on the microstructure and mechanical properties of Ti-6Al-4V to AISI 304 transient liquid phase bonded joint,” *JMADE*, vol. 99, pp. 543–551, 2016.
- [20] M. A. Arafin, M. Medraj, D. P. Turner, and P. Bocher, “Transient liquid phase bonding of Inconel 718 and Inconel 625 with BNi-2: Modeling and experimental investigations,” *Mater. Sci. Eng. A*, vol. 447, pp. 125–133, 2007.
- [21] V. Jalilvand, H. Omidvar, M. R. Rahimpour, and H. R. Shakeri, “Influence of bonding variables on transient liquid phase bonding behavior of nickel based superalloy IN-738LC,” 2013.
- [22] B. Binesh and A. J. Gharehbagh, “Transient Liquid Phase Bonding of IN738LC/MBF-15/IN738LC: Solidification Behavior and Mechanical Properties,” *J. Mater. Sci. Technol.*, vol. 32, pp. 1137–1151, 2016.
- [23] “Brazing.” [Online]. Available: <https://www.britannica.com/technology/brazing>.
- [24] B. Y. J. Wolters, “The Origins of Gold Brazing,” pp. 27–28, 1976.
- [25] “Flux.” [Online]. Available: [https://en.wikipedia.org/wiki/Flux\\_\(metallurgy\)](https://en.wikipedia.org/wiki/Flux_(metallurgy)). [Accessed: 17-Sep-2018].
- [26] J. F. (John F. Lancaster, *Metallurgy of welding*. Abington Pub, 1999.
- [27] Samarth Engineering Works, “No Title.” [Online]. Available: <http://blog.samarthenggworks.com/index.php/advantages-disadvantages-brazing/>.
- [28] Precision Metal Industries, “Torch Brazing - Precision Metal Industries.” [Online]. Available: <http://www.pmiquality.com/torch-brazing/>.
- [29] P. Roberts, “Introduction to Furnace Brazing,” pp. 187–242, 2013.
- [30] J. Matthey and M. Limited, “FURNACE BRAZING A Survey of Modern Processes and Plant,” no. April, pp. 1–26, 1973.
- [31] “Induction brazing - Metal joining services - Bodycote Plc.” [Online]. Available: <https://www.bodycote.com/services/metal-joining/induction-brazing/>. [Accessed: 17-Sep-2018].
- [32] “Frequently Asked Questions : Parfuse Corporation Aluminum Dip Brazing Westbury Long Island New York.” [Online]. Available: <http://www.parfuse.com/faq/index.html>. [Accessed: 17-Sep-2018].
- [33] G. P. Kelkar, “WJM Technologies,” no. 562, pp. 1–5, 2013.
- [34] M. Heitmanek *et al.*, “Laser brazing with beam scanning: Experimental and simulative analysis,” *Phys. Procedia*, vol. 56, pp. 689–698, 2014.
- [35] M. L. Kuntz *et al.*, “Laser brazing in the automotive industry,” *J. Mater. Sci.*, vol. 19, no.

- April, pp. 5305–5323, 2006.
- [36] M. F. Arenas, V. L. Acoff, and R. G. Reddy, “Physical properties of selected brazing filler metals,” *Sci. Technol. Weld. Join.*, vol. 9, no. 5, pp. 423–429, 2004.
- [37] H. S. Flux, “March 7, 1950 R. B. GOODY,” vol. 420, 1950.
- [38] M. Abdelfattah, “An experimental and theoretical study of transient liquid phase bonding of nickel based materials,” 2008.
- [39] D. Jacobson and G. Humpston, *Principles of brazing*. 2005.
- [40] A. W. D. Macdonald and T. W. Eagar, “TRANSIENT LIQUID PHASE BONDING PROCESSES.”
- [41] G. O. Cook and C. D. Sorensen, “Overview of transient liquid phase and partial transient liquid phase bonding,” *J. Mater. Sci.*, vol. 46, no. 16, pp. 5305–5323, 2011.
- [42] O. Aina, “Effects of process parameters on the transient liquid phase bonding of dissimilar materials: in 738 superalloy and cobalt,” 2018.
- [43] T. C. Illingworth, I. O. Golosnoy, V. Gergely, and T. W. Clyne, “PROCEEDINGS OF THE IV INTERNATIONAL CONFERENCE/HIGH TEMPERATURE CAPILLARITY Numerical modelling of transient liquid phase bonding and other diffusion controlled phase changes.”
- [44] Y. Natsume, K. Ohsasa, and T. Narita, “Phase-field Simulation of Transient Liquid Phase Bonding Process of Ni Using Ni-P Binary Filler Metal.”
- [45] I. Tuah-Poku, M. Dollar, and T. B. Massalski, “A study of the transient liquid phase bonding process applied to a Ag/Cu/Ag sandwich joint,” *Metall. Trans. A*, vol. 19, no. 3, pp. 675–686, 1988.
- [46] M. L. Kuntz, “Quantifying Isothermal Solidification Kinetics during Transient Liquid Phase Bonding using Differential Scanning Calorimetry,” p. 214, 2006.
- [47] D.-U. Kim and K. Nishimoto, “Bonding phenomena of transient liquid phase bonded joints of a Ni base single crystal superalloy,” *Met. Mater. Int.*, vol. 8, no. 4, pp. 403–410, Jul. 2002.
- [48] W. Choi, S. Kim, J. Kim, ... G. K.-J. of W. and, and undefined 2005, “Effect of Bonding Temperature and Heating Rate on Transient Liquid Phase Diffusion Bonding of Ni-Base Superalloy,” *koreascience.or.kr*.
- [49] O. Idowu, N. Richards, M. C.-M. S. and, and undefined 2005, “Effect of bonding temperature on isothermal solidification rate during transient liquid phase bonding of Inconel 738LC superalloy,” *Elsevier*.
- [50] O. A. Ojo and M. M. Abdelfatah, “On deviation from parabolic behaviour during transient liquid phase bonding,” *Mater. Sci. Technol.*, vol. 24, no. 6, pp. 739–743, Jun. 2008.
- [51] F. Jalilian, M. Jahazi, R. D.-M. S. and E. A, and undefined 2006, “Microstructural evolution during transient liquid phase bonding of Inconel 617 using Ni–Si–B filler

- metal,” *Elsevier*.
- [52] S. Hadibeyk, B. Beidokhti, S. S.-J. of A. and Compounds, and undefined 2018, “Effect of bonding time and homogenization heat treatment on the microstructure and mechanical properties of the transient liquid phase bonded dissimilar GTD-111,” *Elsevier*.
- [53] V. Jalilvand, H. Omidvar, ... H. S.-M., and undefined 2013, “Microstructural evolution during transient liquid phase bonding of Inconel 738LC using AMS 4777 filler alloy,” *Elsevier*.
- [54] M. Khakian, S. Nategh, S. M.-J. of A. and Compounds, and undefined 2015, “Effect of bonding time on the microstructure and isothermal solidification completion during transient liquid phase bonding of dissimilar nickel-based superalloys,” *Elsevier*.
- [55] Y. Jin, T. K.-M. & Design, and undefined 2012, “Effect of bonding time on microstructure and mechanical properties of transient liquid phase bonded magnesium AZ31 alloy,” *Elsevier*.
- [56] M. Kuntz, Y. Zhou, S. C.-M. and M. T. A, and undefined 2006, “A study of transient liquid-phase bonding of Ag-Cu using differential scanning calorimetry,” *Springer*.
- [57] C. Sinclair, G. Purdy, J. M.-M. and Materials, and undefined 2000, “Transient liquid-phase bonding in two-phase ternary systems,” *Springer*.
- [58] R. Roy, S. S.-T. solid films, and undefined 1993, “The study of diffusion of copper in thin films of silver and Ag-Al alloys as a function of increasing aluminium concentration,” *Elsevier*.
- [59] J. Hirvonen, “Aluminum diffusion in ion-implanted noble metals,” *J. Appl. Phys.*, vol. 52, no. 10, pp. 6143–6146, Oct. 1981.
- [60] N. Sheng, J. Liu, T. Jin, X. Sun, and Z. Hu, “Isothermal solidification stage during transient liquid-phase bonding single-crystal superalloys,” *Philos. Mag.*, vol. 94, no. 11, pp. 1219–1234, Apr. 2014.
- [61] J. Li, P. Agyakwa, C. J.-A. Materialia, and undefined 2010, “Kinetics of Ag<sub>3</sub>Sn growth in Ag-Sn-Ag system during transient liquid phase soldering process,” *Elsevier*.
- [62] C. Houska, F. Dietrich, G. S.-T. S. Films, and undefined 1977, “Time-dependent diffusion coefficients obtained from diffused films: The Cu-Ni system,” *Elsevier*.
- [63] and R. F. M. Lustman, B., “Rate of Growth of Intermediate Alloy Layers in Structurally Analogous Systems,” *AIME TRANS*, vol. 4, no. June 9, pp. 1–26, 1942.
- [64] L. R. Weisberg and J. Blanc, “Diffusion with Interstitial-Substitutional Equilibrium. Zinc in GaAs,” *Phys. Rev.*, vol. 131, no. 4, pp. 1548–1552, Aug. 1963.
- [65] C. Ting, G. P.-J. of T. E. Society, and undefined 1971, “Time-Dependence of Zinc Diffusion in Gallium Arsenide under a Concentration Gradient,” *jes.ecsdl.org*.
- [66] L. D. Hall, “An Analytical Method of Calculating Variable Diffusion Coefficients,” *J. Chem. Phys.*, vol. 21, no. 1, pp. 87–89, Jan. 1953.

- [67] S. Salman, S. Afghahi, A. Ekrami, S. Farahany, and A. Jahangiri, “Philosophical Magazine Effect of bonding parameters on microstructure development during TGTLT bonding of Al7075 alloy Effect of bonding parameters on microstructure development during TGTLT bonding of Al7075 alloy,” 2014.
- [68] T. LIN *et al.*, “Effect of bonding parameters on microstructures and properties during TLT bonding of Ni-based super alloy,” *Elsevier*.
- [69] Y. Z.-J. of materials science letters and undefined 2001, “Analytical modeling of isothermal solidification during transient liquid phase (TLT) bonding,” *Springer*.
- [70] G. DiGiacomo, P. Peressini, and R. Rutledge, “Diffusion coefficient and electromigration velocity of copper in thin silver films,” *J. Appl. Phys.*, vol. 45, no. 4, pp. 1626–1629, Apr. 1974.